Feeder-free culture of naive human pluripotent stem cells retaining embryonic, extraembryonic and blastoid generation potential

Giada Rossignoli[1,#], Michael Oberhuemer[2,3,#], Ida Sophie Brun[4,#], Irene Zorzan[1,15,#], Anna Osnato[5,6], Anne Wenzel[4], Emiel van Genderen[7], Andrea Drusin[1], Giorgia Panebianco[1], Nicolò Magri[1], Mairim Alexandra Solis[5,8], Chiara Colantuono[9], Sam Samuël Franciscus Allegonda van Knippenberg[5,6], Thi Xuan Ai Pham[5,6], Sherif Khodeer[5,6], Paolo Grumati[10,11], Davide Cacchiarelli[10,12,13], Paolo Martini[14], Nicolas Rivron[7], Vincent Pasque[5,6], Jan Jakub Żylicz[4,*], Martin Leeb[2,*] and Graziano Martello[1,*].

Affiliations

1: Department of Biology, University of Padua, Padua, Italy.
2: Max Perutz Laboratories Vienna, University of Vienna, Vienna BioCenter, Vienna, Austria.
3: Vienna BioCenter PhD Program, Doctoral School of the University of Vienna, Medical University of Vienna, Vienna, Austria.
4: Novo Nordisk Foundation Center for Stem Cell Medicine, reNEW, University of Copenhagen, Copenhagen, Denmark.
5: KU Leuven-University of Leuven, Department of Development and Regeneration, Leuven Stem Cell Institute, Leuven, Belgium.
6: KU Leuven Institute for Single Cell Omics (LISCO), Leuven, Belgium.
7: Institute of Molecular Biotechnology of the Austrian Academy of Sciences (IMBA), Vienna BioCenter, Vienna, Austria
8: Gorgas Memorial Institute for Health Studies, Panama, Panama.
9: NEGEDIA S.r.l., Pozzuoli, Italy.
10: Telethon Institute of Genetics and Medicine (TIGEM), Pozzuoli, Italy.
11: Department of Clinical Medicine and Surgery, University of Naples "Federico II", Naples, Italy.
12: Department of Translational Medicine, University of Naples "Federico II", Naples, Italy.
13: Genomics and Experimental Medicine Program, Scuola Superiore Meridionale (SSM, School of Advanced Studies), Naples, Italy.
14: Department of Molecular and Translational Medicine, University of Brescia, Brescia, Italy.
15: Current affiliation: Epigenetics Programme, Babraham Institute, Cambridge, UK.

[#]equal contributions; *Corresponding authors

Abstract

Conventional human pluripotent stem cells (hPSCs) are widely used to study early embryonic development, generate somatic cells, and model diseases, with differentiation potential aligned to a post-implantation epiblast identity. In the past decade, naive hPSCs, representing a pre-implantation stage, have been derived. Naive hPSCs efficiently differentiate towards embryonic and extraembryonic lineages such as trophectoderm, primitive endoderm, and extraembryonic mesoderm, and also self-organize into blastocyst-like structures called blastoids. However, their culture typically relies on mouse embryonic fibroblasts (MEFs), which are variable, resource-intensive, and can confound analyses. We report the long-term maintenance of naive hPSCs in a feeder-free, serum-coated system. We successfully expanded for up to 25 passages 8 different naive hPSCs lines across 5 laboratories. Growth rate, clonogenicity, and gene expression profiles on serum coating were comparable to MEF-based cultures, but serum coating eliminated fibroblast contamination. Naive hPSCs cultured on serum exhibited more efficient germ layer specification, retained trophectoderm potential and high blastoid formation efficiency. Exome sequencing revealed fewer mutations in serum-cultured cells, and mass spectrometry identified extracellular matrix proteins such as vitronectin, fibronectin, and collagens in the serum coating. Overall, serum coating offers a scalable, cost-effective and therefore widely applicable alternative for naive hPSC culture, maintaining developmental potential, reducing DNA mutations, and eliminating MEF-related confounding factors. We believe serum coating will expand the use of naive hPSCs to large-scale studies and facilitate the investigation of mechanistic insights into developmental and disease modelling.

Keywords:

Naive pluripotency; blastoids; extraembryonic lineages, extracellular matrix.

Introduction

The derivation of human pluripotent stem cells (hPSCs) has transformed the stem cell field. Given their potential to self-renew and differentiate into specialised cell types, there have been high expectations for their use in biological and medical research. hPSCs were first derived from the inner cell mass (ICM) of *in vitro* fertilised embryos (Human Embryonic Stem Cells, hESCs), and cultured in serum-based media on a feeder layer of inactivated mouse embryonic fibroblasts (MEFs)[1], following the methods developed for ICM-derived mouse ESCs (mESCs)[2]. However, it soon became clear that the self-renewal requirements of hESCs and mESCs were different. Undifferentiated mESCs could be maintained in feeder-free conditions in the presence of leukaemia inhibitory factor (LIF) and foetal bovine serum (FBS) on gelatin-coated plates[3,4]. Subsequently, two inhibitors (2i), the MEK inhibitor PD0325901 and the GSK3 inhibitor CHIR99021 were shown to promote efficient mESCs self-renewal in the absence of feeders[5,6]. The combination of 2i and the cytokine LIF (2iL) resulted in more robust proliferation, increased oxidative phosphorylation and genome hypomethylation[7–9]. Since 2007, when hPSCs were reprogrammed from human somatic cells (human induced pluripotent stem cells, hiPSCs) by overexpressing a cocktail of transcription factors (OCT4, SOX2, KLF4 and c-MYC from Takahashi *et al*[10], and OCT4, SOX2, NANOG and LIN28 from Yu *et al*[11]), hundreds of lines of hPSCs have been derived. Surprisingly, hPSCs were found not responsive to 2iL[12]. In contrast, they can be cultured without feeders on Matrigel or vitronectin-coated plates in Essential 8 (E8) or mTeSR media, both based on FGF2 and TGFβ supplementation[13–15].

Although hESCs, like mESCs, are derived from pre-implantation blastocysts, they do not reside in a naive state of pluripotency and rather correspond to primed mouse ESCs derived from post-implantation epiblast (mEpiSCs), regarding growth factor dependence and transcriptional and epigenetic regulation[16–19]. Furthermore, hESCs (and hiPSCs) exhibit lower expression of pluripotency genes such as *NANOG*, *KLF4*, *KLF17*, *DPPA3*, and *DPPA5* when compared to the human naive epiblast[20]. The ability to convert mEpiSCs into mESCs provided a paradigm for the generation of naive human stem cells. This led different research groups to first derive naive hPSCs in 2iL by overexpressing transcription factors associated with naive pluripotency[12,21], and later to implement more specific culture conditions and genetic manipulations[22–25]. Since then, naive hPSCs have been successfully derived from human blastocysts and somatic cell reprogramming by transient gene overexpression or chemical resetting from primed hPSCs in various media[26–30]. Successful maintenance of human naive pluripotency *in vitro* in a transgene-independent manner and in serum-free medium was initially achieved by culture optimisation starting from 2iL conditions[24,25]. The addition of Gö6983, a protein kinase C (PKC) inhibitor, previously shown to suppress also mESCs differentiation[31], combined with a lower concentration of CHIR99021 (t2iLGö) was beneficial in maintaining compact colonies with morphology and proliferation of naive hESCs[24]. Later on, GSK3 inhibition was shown to be dispensable

for the maintenance and resetting of naive hPSCs, so CHIR99021 was omitted and the tankyrase inhibitor XAV939 (PXGL) was added to achieve more robust and stable naive features[32]. A high-throughput chemical screen identified a combination of compounds, including the alternative GSK3 inhibitor IM12, the BRAF inhibitor SB590885, the SRC inhibitor WH-4-023, and the ROCK inhibitor Y-27632, supplemented with FGF and Activin A that synergise with PD0325901 and LIF to support the expansion of naive hPSCs (5i/L/AF)[25]. The addition of the JNK inhibitor SP600125 (6i/L/A) has been reported to increase the efficiency of naive hPSCs induction from the primed state[25]. Meanwhile, chemically defined conditions termed NHSM (naive human stem cell medium) were developed, in which 2iLGö was supplemented with p38 inhibitor SB203580 or BIRB796, JNK inhibitor SP600125, ROCK inhibitor Y-27632, bFGF and TGF-β1[23].

The derivation of naive hPSCs has broadened the potential applications of human embryonic stem cells. Consistent with the fact that their transcriptomic state reflects a developmental state similar to the blastocyst stage epiblast rather than post-implantation epiblast, naive hPSCs exhibit a broader differentiation potential compared to primed hPSCs, enabling efficient differentiation into extraembryonic tissues, including trophectoderm (TE)[33–36], primitive endoderm (PrE)[37,38], and extraembryonic mesoderm[39], three lineages previously inaccessible for *in vitro* studies. Furthermore, naive hPSCs can aggregate and generate 3D blastocyst-like structures composed of the three founding lineages as a model to study human implantation and peri-implantation development[40–42]. Naive hPSCs are characterised by global genomic hypomethylation compared to primed cells[43] - like mESCs[9] - and biallelic expression of multiple imprinted genes[44,45]. Naive hPSCs also use a bivalent metabolic system with a greater reliance on oxidative metabolism, whereas primed hPSCs are almost exclusively glycolytic[24,25,46,47], as reported for naive mESCs[8].

A major hurdle for studying the human naive state is that, unlike the mouse naive and human primed states, they are still routinely cultured on MEFs. In addition to the experimental cost and time involved, the quality of culture on feeders has been shown to depend on numerous other factors such as embryo age, passage number of MEFs and their genetic background, all of which affect gene expression and factor release from MEFs themselves, as well as stem cells proliferation and colony formation[48–51]. The exchange of signals between feeders and PSCs, some of which are still unknown, undoubtedly prevents a stringent control of the system and makes it more difficult to understand the best conditions and underlying biological pathways necessary for maintaining pluripotency *in vitro*, with implications also in downstream analyses and applications of these cells. There have been extensive efforts to eliminate feeders from naive hPSC cultures. However, to this date, they have not been widely adopted for multiple reasons. A 3D culture system based on Matrigel allows for a robust expansion of naive hPSCs in PXGL[52]. While it allows for efficient 3D differentiation, it is time- and resource-intensive as a routine culture method. Reduced proliferation was reported if MEFs were replaced with Matrigel or laminin-511 coating in t2iLGö medium in 2D[24]. Media formulations with extensive addition of inhibitors

130 allowed for robust expansion of hPSCs on Matrigel or Vitronectin-coated plates (FINE, NHSM and
131 RSeT, a commercial medium based on NHSM)[23,53]. However, these inhibitors affect the morphology[53]
132 or stabilise a transcriptional state of hPSCs distinct from naive cells routinely used in blastoid
133 formation[23,27]. Consequently, the routinely used conditions for naive hPSCs expansion and blastoid
134 generation rely on MEFs[40–42].

135 The addition of serum to cell culture media has been used to improve cell adhesion since the first half
136 of the last century[54–56]. Analysis of serum composition led to the discovery of the extracellular matrix
137 (ECM) protein vitronectin[57], together with fibronectin[58]. Murine EpiSCs can be expanded efficiently on
138 FBS-coated plates[16]. Interestingly, mESCs cultured on serum-coated substrates in the presence of LIF
139 maintain the expression of *OCT4* and grow as round cells in small colonies[59]. Moreover, while mESCs
140 strongly attach when converted from 2iL to serum/LIF, cells in a serum-containing medium might have
141 attachment problems when converted to serum-free 2iL, and the addition of a small amount of FBS in
142 2iL generally enhances adhesion[60]. Furthermore, conventional hPSCs have been successfully grown on
143 serum-coated substrates without feeders[61].

144 In this study, we observed, across 5 laboratories, that naive hPSCs of both induced and embryonic
145 origins can be easily adapted to a feeder-free, serum-based coating in PXGL. Cells grown on serum
146 coated culture dishes retain a naive pluripotency gene expression signature, and a proliferation rate and
147 clonogenic capacity similar to the original lines on MEFs, without acquiring pathogenic-associated
148 mutations. In addition, naive hPSCs cultured on serum coating retain full differentiation potential
149 towards both extra-embryonic and embryonic tissues as well as the capacity to self-assemble into
150 blastoids.

151 # Results

152 ## Naive hPSCs spontaneously adapt to serum coating

153 Naive hiPSCs directly reprogrammed from somatic cells[30] (HPD06 and HPD03) were plated in PXGL
154 medium on dishes coated with 10% FBS diluted in DMEM (i.e. serum coating) without MEFs. Feeder-
155 free converted cells retained their distinctive dome-shaped morphology (Supplementary Figure 1A) and
156 expressed general pluripotency (*POU5F1/OCT4* and *NANOG*) and naive-specific markers (*TFCP2L1*,
157 *KLF4* and *KLF17*) at comparable or even higher levels than cells cultured on MEFs, as well as low or
158 undetectable expression of primed genes *OTX2* and *ZIC2* (Figure 1A). Comparable protein levels of
159 naive markers KLF17 and TFCP2L1, and the general pluripotency markers OCT4 and NANOG were
160 observed in feeder-free and MEFs cultured cells (Figure 1B, left, and Supplementary Figure 1B). Two
161 naive PSC lines (HPD06 and HPD03) displayed a decrease in the proliferation rate (Supplementary
162 Figure 1D) and clonogenic capability (Supplementary Figure 1E) when plated at low density on serum
163 coating in comparison to the same cell lines on MEFs during the first 4 passages of the conversion.
164 Upon long-term culture in feeder-free conditions, these hPSC lines retained the dome-shaped
165 morphology (Figure 1C, left) and recovered growth rate and clonogenicity to levels comparable to the
166 same cell line cultured on MEFs (Figure 1D-E). We conclude that serum coating allows for the
167 maintenance of naive pluripotency markers and the long-term expansion of naive hiPSCs.

168 Prompted by these results, we decided to test extensively whether serum coating could be used for naive
169 PSC lines of different origin (i.e. reprogramming of fibroblasts, resetting of conventional PSCs and
170 embryo-derived), of both sexes and in different laboratories. Furthermore, we reasoned that an extensive
171 test of the differentiation potential should be performed, including both embryonic and extraembryonic
172 lineages, to test if serum coating allows for the maintenance of *bona fide* naive PSCs (Figure 1F). We
173 successfully converted 8 human naive PSC lines in 5 different laboratories to feeder-free conditions
174 (Table 1). They all displayed comparable expression of nuclear (OCT4 and NANOG) and naive markers
175 (KLF17 and SUSD2) (Figure 1B, G and Supplementary Figure 1C, F), with dome-shaped morphology
176 and robust expansion (Figure 1C). Although only HPD06 and HPD03 lines exhibited a lag phase before
177 complete adaptation, we have not experienced a line failing to convert to serum coating in PXGL.

178 We concluded that naive hPSCs spontaneously adapt to the feeder-free culture on serum coating in
179 PXGL without additional treatment or genetic manipulation.

180 ## Proteomics analysis of serum composition reveals abundant ECM proteins

181 We wondered how serum coating could sustain the attachment and growth of naive hPSCs. Previous
182 studies identified Vitronectin as a component of serum accounting for its capacity to promote cell

183 adhesion[57]. Therefore we assessed the composition of the coating through a label-free quantitative
184 proteomics analysis. The entire list of identified proteins was screened and annotated for matrisome and
185 matrisome-associated macromolecules using the Matrisome AnalyseR tool from The Matrisome
186 Project[62]. Of the 850 proteins detected in serum coating, 183 (more than 20%) were classified as "Core
187 matrisome" or "Matrisome-associated" hits. ECM glycoproteins and ECM-affiliated proteins and
188 regulators accounted for the majority of the hits in these two categories (Figure 2A). The analysis of the
189 top 100 most prevalent proteins in serum coating showed that Fibronectin, Vitronectin, Laminin, and
190 several Collagens were present (Figure 2B).

191 Therefore, the serum contains a mixture of ECM proteins previously reported to support conventional
192 human PSCs[13–15].

193 Serum coating does not induce genetic variations in naive hPSCs

194 Several studies demonstrated that conventional hPSCs can acquire genetic changes during long-term *in*
195 *vitro* culture, which commonly include mutations in cancer-associated genes, especially TP53[63,64]. We
196 analysed specifically the two naive iPSC lines (HPD06 and HPD03) that required some passages to
197 recover their proliferation rate on serum (Figure 1D), wondering whether they acquired mutations in
198 hotspot genes during the adaptation. We collected genomic DNA from HPD06 and HPD03 cultured for
199 more than 2 months after conversion to serum coating and from the same lines kept on MEFs (Figure
200 3A) and deep sequenced exomes (more than 600 million reads, 1000x independent base coverage). The
201 comparison with the reference genome identified a total of 1649 shared variants (SNVs, indels, and
202 CNVs) in protein-coding regions between HPD06 naive hPSCs cultured on MEFs and serum, likely
203 accumulated during derivation and previous culture on MEFs (Figure 3B, left Venn diagrams).
204 However, HPD06 continuously cultured on MEFs accumulated 936 variants, contrary to the 356
205 variants specifically detected in the same line cultured on serum. Similarly, more variants were detected
206 in HPD03 naive hPSCs on MEFs than in the same line converted to serum coating (509 and 311,
207 respectively; Figure 3B, top Venn diagrams). We then grouped protein-coding variants according to
208 their clinical impact (tier I, strong significance; tier II, potential clinical significance; tier III, unknown
209 clinical significance; and tier IV, benign or likely benign)[65]. For both HPD06 and HPD03, no Tier I
210 alterations were identified and Tier IV represented the vast majority of detected variants (Figure 3B,
211 bottom bar plots). Interestingly, for both naive lines, the culture on MEFs showed an accumulation of
212 Tier III variants compared to serum coating (Figure 3B, bar plots). Few cancer-related genes previously
213 reported as commonly mutated in conventional hPSCs showed only Tier IV benign or likely benign
214 alterations (*FAT1*, *ASXL1* and *NF1*)[64]. No genetic alteration was found for *TP53*, a predominantly
215 mutated gene during *in vitro* culture[63,64].

216 Overall, culturing naive hPSCs on serum coating did not lead to pathogenic mutations. Moreover,
217 mutation rates of naive lines cultured on serum were lower compared to MEFs-cultured cells.

218 Naive hPSCs on serum coating maintain the transcriptomic profile and lack
219 of gene imprinting

220 To further characterise the naive features of hPSCs on serum, we compared the transcriptome of our
221 naive hPSCs cultured on MEFs and serum coating with a panel of published transcriptomes spanning
222 human naive and primed PSCs, TSCs and fibroblasts. RNA-seq data confirmed a distinct global
223 expression profile of our naive hPSC lines compared with primed hPSCs, TSCs and fibroblasts, as they
224 fall together within the main naive cluster (Figure 3C). Gene expression analysis confirmed robust
225 induction of several core and naive specific pluripotency genes (Figure 3D), and low to undetectable
226 expression of primed-specific markers, in line with published transcriptomes. Generally, primed and
227 naive hPSCs cultured on MEFs showed variable expression of fibroblast markers, possibly due to MEF
228 contamination in collected cells (Figure 3D and Supplementary 2C). Fibroblast markers were barely
229 detectable in naive lines cultured on serum.

230 It has been observed that mitochondrial activation and metabolic realignment occur concurrently with
231 the generation and stabilisation of naive hPSCs[24]. Mouse ESCs use oxidative phosphorylation, while
232 mEpiSCs and hPSCs are mostly glycolytic and have low ability for mitochondrial respiration[46]. We
233 collected the list of oxidative phosphorylation genes from KEGG (ko00190 pathway;
234 https://www.genome.jp/kegg/pathway.html) and added the complex IV cytochrome c oxidase (COX)
235 genes. In naive hPSCs, we observed an increase in the expression of most genes involved in oxidative
236 phosphorylation (Supplementary Figure 2A). Furthermore, in agreement with previously published
237 data[24,46], the expression of most of the COX genes was decreased in primed hPSCs compared to naive
238 hPSCs, both on MEFs and serum coating.

239 Previous studies reported biallelic expression of some imprinted genes in human naive PSCs[44,45,66].
240 Therefore, we analysed our bulk RNA-Seq samples with BrewerIX[45], running the analysis with the
241 complete pipeline. We detected a significant biallelic expression of H19 and ZIM2/PEG3 specifically
242 in all naive hiPSCs, either on serum or MEFs, but not in primed hiPSCs (Supplementary Figure 2B), as
243 previously reported[44,67]. Overall, naive cells displayed similar allelic expression of imprinted genes on
244 serum and MEFs.

245 We concluded that naive hPSCs cultured on serum coating maintain their distinctive transcriptome
246 profile without significant alterations compared to naive hPSCs cultured on MEFs.

247 **Serum-adapted naive hPSCs faithfully recapitulate embryonic**
248 **differentiation trajectories**

249 Upon withdrawal of self-renewal cues, naive hESCs exit the naive pluripotent state. Before gaining the
250 ability to commit to embryonic cell fates, they need to undergo a process termed capacitation[68].
251 Capacitation requires approximately eight to ten days, consistent with the timing between the blastocyst
252 and the pre-gastrulation post-implantation embryo *in vivo*. Hence, to assess the capacitation and
253 differentiation potential of serum-cultured naive hPSCs (Figure 1F), we subjected them to a variety of
254 differentiation conditions. Changes in morphology were equivalent between naive hPSCs cultured on
255 MEFs or serum coating, across multiple differentiation media (Supplementary Figure 3A). Furthermore,
256 expression of naive specific markers (*TFCP2L1*, *KLF4* and *NANOG*) was downregulated while
257 expression of primed markers (*SALL2*, *CDH2* and *ZIC2)* was induced during the exit from naive
258 pluripotency irrespective of whether hESCs were maintained on MEFs or serum before the induction
259 of differentiation (Figure 4A). Consistently, naive transcription factors downregulation and primed
260 marker upregulation were also observed in Shef6 hESCs cultured on serum coating inducing
261 capacitation (Figure 4B) and were confirmed at the protein level (Supplementary Figure 3B).

262 To further characterise gene expression behaviour during capacitation, we explored transcriptome
263 changes throughout an eight-day differentiation time course in various conditions: unsupplemented
264 N2B27, N2B27 supplemented with TNKS1/2 inhibition (XAV)[68] or FGF2-ActivinA-XAV (FAX), or
265 E8 or mTeSR, which contain FGF and Activin signalling ligands. All differentiation was induced from
266 naive Shef6 hESCs cultured on serum. We firstly noted that differentiation time points, rather than
267 medium conditions, had the largest impact on clustering (Figure 4C) and that the Spearman correlation
268 between the same time points of different conditions was high (Supplementary Figure 3C).
269 Consistently, expression kinetics of *KLF4* and *ZIC2* were equivalent between conditions (Figure 4D).
270 Comparison with published data for MEF-cultured H9 and HNES1 naive hESC lines differentiating
271 with XAV[68], showed that Shef6 naive hESCs cultured on serum coating followed the same trajectory
272 as H9 and HNES1 hESCs cultured on MEFs before capacitation (Figure 4E), and have similar
273 expression patterns for known pluripotency genes (Figure 4F). We also noted that the presence of XAV
274 had no discernable effect regarding gross gene expression or proliferation compared to capacitation in
275 N2B27 alone. We surmise that the gene expression programme accompanying capacitation is not
276 affected by the substrate used for culture.

277 We next benchmarked our *in vitro* capacitation system starting from serum-coated naive hPSCs by
278 comparing our RNA-seq time course data to data of human *ex vivo* cultured pre- and peri-implantation
279 embryos[69]. Principal component analysis showed a striking alignment between our *in vitro* capacitation
280 system and embryo data (Figure 4G). This is reflected in a clear correlation between differentiation-

281 induced gene expression changes *in vitro* and *in vivo* at both the global transcriptome (Supplementary
282 Figure 3D), and the individual pluripotency marker level (Figure 4F and Supplementary Figure 3E-F).

283 Taken together, these findings demonstrate that serum-adapted hPSCs progress through the
284 developmental states of pluripotency at least as well as feeder-dependent hPSCs and that this model can
285 generate results compatible with *in vivo* embryonic development.

286 Naive hPSCs on serum coating efficiently differentiate to the three primary 287 germ layers and TSCs

288 After confirming that naive hPSCs cultured on serum can exit pluripotency under different conditions
289 with a progression similar to that of the same cell line cultured on MEFs (Figure 4 and Supplementary
290 Figure 3), we wondered if naive hPSCs cultured in feeder-free conditions still retain the capacity to
291 efficiently differentiate into embryoid bodies (EBs) composed of the three germ layers (Figure 1F).
292 Capacitated hPSCs from naive cells previously cultured on MEFs or serum coating were aggregated in
293 3D and let spontaneously differentiate for 14 days (Figure 5A). EBs derived from both conditions
294 showed an upregulation of germ layer markers compared to capacitated cells (Figure 5B). We conclude
295 that naive hPSCs cultured on serum efficiently capacitate and differentiate to the three germ layers with
296 similar or even better efficiency compared to naive hPSCs previously cultured on MEFs.

297 Naive hPSCs cultured on MEFs can also promptly differentiate toward TSCs when exposed to TSC
298 medium[34,35,70]. Therefore, we assessed whether naive hPSCs cultured on serum coating still retain this
299 capacity. We obtained TSCs in a few passages from naive hiPSCs stably cultured in both conditions,
300 which showed indistinguishable morphology (Figure 4C) and similar downregulation of naive genes
301 *TFCP2L1* and *KLF17* and upregulation of TSC genes *GATA3* and *GATA2* (Figure 5D and
302 Supplementary Figure 4A). Consistently, the GATA3 signal was detected by immunofluorescence at a
303 comparable level to stable naive-derived TSCs (passage 15), while KLF17 and OCT4 were undetectable
304 (Figure 5E and Supplementary Figure 4B). Several genes (e.g. *TFAP2A*, *KRT7,* and *GATA3* and *GATA2*
305 to a lesser extent) are shared between TSCs and amnion, as early amniogenesis has been reported to
306 occur via a trophectoderm-like route[71]. Therefore, we wondered if TSCs derived from naive hiPSCs
307 cultured on serum retain the same low expression of amnion markers of naive hiPSCs cultured on MEFs.
308 We previously reported that BAP medium-treated primed hPSCs showed increased expression of
309 *GATA3* together with amnion markers *IGFBP3* and *BAMBI*[72]. Therefore, we exposed primed
310 Keratinocytes induced Pluripotent Stem Cells (KiPS) to BAP medium and observed a cell morphology
311 consistent with previous reports[36,72,73] and completely distinct from our naive hiPSCs-derived TSCs
312 (Supplementary Figure 4C, left and Figure 4A). We analysed the expression of the amnion markers[35,70]
313 and detected lower expression of *IGFBP3* and undetectable expression of *BAMBI* in TSCs derived from
314 naive hiPSCs cultured both on MEFs and serum coating compared to BAP-treated cells (Supplementary

315 Figure 4C). We concluded that naive hiPSCs cultured in both conditions readily differentiate to *bona*
316 *fide* TSCs with similar efficiency.

317 Naive hPSCs on serum coating efficiently self-organize into blastoids

318 Previous studies have reported that naive hPSCs when aggregated are able to self-organize into
319 blastoids. Blastoids are integrated stem cell embryo models reminiscent of the human blastocyst[40–42].
320 Indeed, such structures robustly specify an outer layer of TE-like cells encompassing the pluripotent
321 epiblast (EPI)-like cells and rare PrE-like cells. To test if naive hPSCs cultured on serum retain this
322 unique characteristic, we optimised the Kagawa *et al*[41,74] blastoid induction protocol for naive H9 hESCs
323 (Table 1). When passaged at high densities, naive H9 hESCs cultured on serum coating were able to
324 aggregate in AggreWells and form blastoid structures without the need for the time-consuming plastic
325 attachment step typically used to deplete MEFs and differentiated cells from the cultures (Figure 6A,
326 top). Blastoids derived from naive H9 hESCs cultured on serum coating showed comparable cavitation
327 efficiency, diameter, and rate of single cavities to blastoids derived from naive hESCs cultured on
328 feeders (Figure 6A, top and Supplementary Figure 5A). Comparable efficiency of blastoid formation
329 was observed also using the male naive hiPSC line KOLF2.1J cultured on MEFs or serum coating
330 (Figure 6A, bottom). Immunofluorescence analysis validated that these structures contain TE-like
331 (GATA2/3 or CDX2), EPI-like (NANOG or OCT4), and rare PrE-like cells (GATA4 and SOX17)
332 (Figure 6B). Comparable results were obtained with naive HNES1 hESCs and the female naive hiPSC
333 line SCTi003-A (Supplementary Figure 5B-C). This analysis confirmed that naive hESCs and hiPSCs
334 cultured on serum-coated dishes are able to robustly self-organize into blastoids.

335 To validate these cellular identities, we performed 10x scRNAseq on day 5 blastoids derived from naive
336 H9 hESCs cultured on serum-coated dishes. This analysis showed two populations of cells on the
337 UMAP (Figure 6C). Based on the expression of key marker genes, the two populations were annotated
338 as TE-like and EPI-like cells (Figure 6D-E). Notably, TE-like cells expressed a wide range of
339 trophoblast markers (e.g., *GATA3, NR2F2, GATA2*) but not those of the amnion (e.g., *ISL1, TFAP2B*)
340 or other off-target lineages (Figure 6D-E, Supplementary Figure 5D). Similarly, EPI-like cells
341 expressed both core (e.g., *POU5F1, NANOG*) and naive pluripotency markers (e.g., *DPPA5, DNMT3L*)
342 but not those associated with primed pluripotency (e.g., *OTX2, ZIC2*) (Figure 6D-E, Supplementary
343 Figure 5D). Previous reports have shown that PrE-like cells are very rarely specified during blastoid
344 induction[41]. Consistent with this finding, we only observed sporadic individual cells expressing the PrE
345 marker *GATA4*, and no Seurat cluster contained a significant number of PrE-like cells (Supplementary
346 Figure 5D-E). To further validate these annotations, we integrated our data with embryo reference
347 datasets (Supplementary Figure 5F)[20,40,69,75–78]. Notably, our single-cell dissociation protocol
348 disproportionately fragilises the TE-like cells; therefore, scRNA-seq was only used to verify cellular
349 identities rather than to quantify the proportion of individual lineages. Nevertheless, our analysis

350 confirmed that cluster 4 is predominantly composed of TE-like cells, while the remaining clusters retain
351 EPI identity (Figure 6F, Supplementary Figure 5F-G). This analysis confirmed that the blastoids contain
352 *bona fide* TE-like and EPI-like cells. Overall, the formation of blastoids was achieved using 4 lines in
353 3 different laboratories, demonstrating the robustness of the protocols and their potential for wide
354 adoption in the community.

355 Overall, feeder-free naive hESCs, when aggregated, robustly self-assemble into blastoids containing
356 cells with appropriate lineage identities.

Discussion

Expansion of human naive PSCs on a layer of inactivated MEFs has several limitations. Production of MEFs requires the sacrifice of mice, which contrasts with the 3Rs principles for the ethical use of animals in research. MEF production is also time-consuming and expensive, limiting the range of application of human naive PSCs. Indeed, both mESCs and conventional hPSCs became widespread models only once feeder-free conditions were developed[3,13–15].

The use of MEFs brings an additional hurdle, which is the co-culture of non-human cells with hPSCs. The former might appear as contaminants in global analyses of the latter, as suggested by our analyses of several RNA-sequencing datasets revealing widespread expression of fibroblast markers (Supplementary Figure 2C). Furthermore, the two cell populations might affect each other in a non-controllable manner.

Conventional hPSCs can be expanded without feeders on plates coated with recombinant ECM proteins, such as fibronectin and vitronectin[14,15]. Alternatively, solubilised basement membrane matrixes, commercialised as Matrigel or Geltrex, can be used[13]. However, these substrates have been tested for human naive PSC expansion with only limited success. In some cases (i.e. laminin) only short-term expansion could be achieved, while in others (i.e. Matrigel) stable expansion could be achieved only with additional inhibitors in the media[23,24,53].

Importantly, these substrates are expensive and range from 0.5 to 2 Euros/cm^2. In contrast, the cost of using serum coating is reduced by two orders of magnitude to around 0.5 cents/cm^2, while allowing for long-term expansion without requiring any additional changes in media formulation or culture regime.

For all these reasons, serum-coating represents a significant improvement over current methodologies, allowing for the widespread use of naive hPSCs for several applications, such as large-scale screenings, epigenetic and metabolic profiling, and the generation of embryo models such as blastoids. Expansion of naive hPSCs on serum resulted in a streamlined blastoid protocol, which worked in multiple laboratories with multiple cell lines, with an efficiency as high as feeder-based protocols.

A recent study showed that human naive PSC colonies are surrounded by laminins and collagens[52], which are, at least in part, produced by naive hPSCs themselves. However, this autocrine ECM protein production is not sufficient for PSC expansion, as either MEFs or exogenous substrates are needed. Our proteomic analysis of the FBS coating allowing for human naive PSC expansion revealed the presence of several Collagens, Laminins, together with Vitronectin and Fibronectin. We, therefore, speculate that this combination of ECM proteins is crucial for naive hPSC expansion, but future functional studies will be needed to tease out the contribution of each individual ECM protein.

Implementing our approach requires batch testing of serum, a standard procedure for over 40 years, also required for the culture of mESCs with serum-based media[79]. Indeed, in our experience, FBS batches

allowing robust expansion of mouse ESCs all worked well for providing growth substrates for naive hESCs.

We also observed that harsh treatments, such as growth at clonal density after fluorescence-activated cell sorting in the presence of antibiotics are better tolerated on feeders. Thus, some procedures, such as genomic engineering, might be performed preferably on MEFs. Genomic engineering on mESCs via homologous recombination has been performed on feeders for similar reasons[80–84]. We note that shuttling serum-adapted hESCs between serum coating and MEFs works without the need for re-adaptation to feeder-free conditions.

Finally, this manuscript represents a joint effort of several laboratories routinely working with naive hPSCs. Once a methodology was identified by one lab, reagents and protocols were shared with other labs, resulting in extensive testing of multiple lines for different applications before publication. This constructive and cooperative approach allowed us to quickly build trust in our methodology, thanks to the testing performed in parallel by 5 labs.

Materials and Methods

Culture of hPSCs

Naive hiPSCs HPD06 and HPD03 were previously generated by direct reprogramming from somatic cells as described in[30] were cultured on mitotically inactivated mouse embryonic fibroblasts (MEFs; DR4 ATCC) or serum coating in PXGL medium [32] at 37°C, 5% CO_2, 5% O_2. The PXGL medium was prepared as follows: N2B27 (DMEM/F12 [Gibco 11320074], and Neurobasal in 1:1 ratio [Gibco 21103049], with 1:200 N2 Supplement [Gibco 17502048], and 1:100 B27 Supplement [Gibco 17504044], 2 mM L-glutamine [Gibco 25030024], 0.1 mM 2-mercaptoethanol [Merck Sigma Aldrich M3148]) supplemented with 1 µM PD0325901 (Axon Medchem 1408), 2 µM XAV939 (Axon Medchem 1527), 2 µM Gö6983 (Axon Medchem 2466) and 10 ng/ml human LIF (Qkine Qk036). Serum coating medium was composed of cold 10% Fetal Bovine Serum [Gibco A5256701 or Sigma-Aldrich F7524 or Biowest S1600] in DMEM high glucose [Gibco 41965039]. After adding 2ml of serum coating solution to each well of a 6-well plate, plates were incubated overnight at 37°C, rinsed once with PBS without MgCl2/CaCl2 (Merck Sigma Aldrich D8537) before plating the cells. Cells were passaged as single cells every 3-4 days at a split ratio of 1:3 or 1:4 following dissociation with TrypLE (Gibco 12563029) for 3 minutes at room temperature. 10 µM ROCK inhibitor (ROCKi, Y27632, Axon Medchem 1683) was added to the naive medium for 24 hours after passaging. For the feeder-free conversion, naive hiPSCs HPD06 and HPD03 stably cultured on MEFs were collected with ReLeSR (STEMCELL Technologies 100-0483). Cells were first incubated for 2 minutes at room temperature, followed by another 5 minutes at 37°C after the complete aspiration of the reagent. Cells were collected by carefully washing the well with fresh PXGL medium adding 10 µM ROCKi and were plated on feeder-free plates coated with serum at a 1:1 to 1:2 ratio.

Naive hESCs H9[1] from Leeb's group and Shef6[85] were cultured on mitotically inactivated DR4 MEFs or serum coating (DMEM high glucose [Sigma-Aldrich D5671] and 10% FBS (Sigma-Aldrich F7524 or Biowest S1600) in PXGL at 37°C, 5% CO_2, 5% O_2. Cells were passaged every 3-4 days at a split ratio up to 1:12 using Accutase (Merck Sigma Aldrich A6964) for 5 minutes at 37°C. 10 µM ROCK inhibitor was added to the naive medium for 24 hours after passaging. Naive H9 hESCs from Zylicz's group were instead passaged at a split ratio up to 1:6 using TrypLE (Gibco 12563029) for 3 minutes at 37°C.

Naive KOLF2.1J[86] and SCTi003-A (STEMCELL Technologies 200-0511) hiPSCs from Rivron's group were cultured on 0.1% gelatin-coated plates including a feeder layer of irradiated MEFs or serum coating (DMEM high glucose and 10% FBS (Gibco A5256701)) in PXGL at 37°C, 5% CO2, 5% O2. Cells were passaged every 3-4 days in a ratio of 1:6 following dissociation with Accutase (Merck Sigma Aldrich A6964) for 5 minutes at 37°C. 10 µM ROCK inhibitor was added for 24 hours after passaging.

441 Naive H9 hESCs from Pasque's, SIG-1 hiPSCs (Sigma-Aldrich iPSC EPITHELIAL-1-IPSC0028), and
442 HNES1 hESCs[26] were cultured on MEFs or serum coating (10% Fetal Bovine Serum [Gibco 10270] in
443 DMEM high glucose [Gibco 41966029]) in PXGL at hypoxia conditions in 5% O2 and 5% CO2
444 incubator under humidified conditions at 37°C. Cells were passaged every 3 days at a split ratio up to
445 1:10 by single-cell dissociation with Accutase (Sigma-Aldrich, A6964-100ML) for 5 minutes at 37°C.
446 10 µM ROCK inhibitor was added to the naive medium for 24 hours after passaging.
447 Human primed KiPS[24] were cultured on pre-coated plates with 0.5% growth factor-reduced Matrigel in
448 E8 medium, made in-house according to [15], at 37°C, 5% CO2, 5% O2. Cells were passaged every 3–
449 4 days at a split ratio of 1:8 following dissociation with 0.5 mM EDTA (Invitrogen AM99260G) in PBS
450 without $MgCl_2$/$CaCl_2$.
451 Primed hESCs H9 from Leeb's group (WiCell#WA09) and re-primed Shef6 were maintained feeder-
452 free on plates pre-coated with 1 % (v/v) Geltrex: (Gibco A1413302) in E8 flex (Gibco A2858501)
453 supplemented with 1 % (v/v) Pen/Strep at 37°C, 5% CO2, 5% O2. Following dissociation with Versene
454 (Gibco 15040-033) at room temperature for 5 minutes, cells were passaged every 3-4 days at a split
455 ratio of 1:6.
456 Primed hESCs H9 from Pasque's group were grown in pre-coated geltrex tissue culture at normoxia
457 conditions and under humidified conditions at 37°C in complete E8Flex medium (Thermo Fisher,
458 A2858501). Cells were dissociated into clumps every 5–6 days by incubating 5 min at room temperature
459 in Accutase and passaged at a split ratio of 1:12. 10 µM ROCK inhibitor was added to the naive medium
460 for 24 hours after passaging.
461 All cell lines were routinely checked for mycoplasma and tested negative (Euroclone EMK090020 or
462 Mycoplasma check Service from Eurofins).

463 Capacitation of naive hPSCs

464 Naive hiPSCs HPD06 stably cultured on MEFs or serum coating were capacitated following
465 Rostovskaya *et al*[68] protocol with minor modifications. Briefly, cells were dissociated with TrypLE,
466 and 5×10^4 cells/cm^2 were seeded on a 6-well plate pre-coated with 0.5% growth factor-reduced Matrigel
467 in E8 medium with 10 µM ROCKi (day 0). From day 1 to day 6 cells were cultivated in N2B27 with 2
468 µM XAV939. From day 6 onward the medium was changed to XAF (N2B27 supplemented with 2 µM
469 XAV939, 20 ng/ml Activin A [Qkine Qk001] and 10 ng/ml FGF2 [Qkine Qk002]).
470 Naive hESCs Shef6 and H9 stably cultured on MEFs or serum coating were capacitated following a
471 modified version of the Rostovskaya *et al*[68] protocol. Briefly, cells were dissociated with Accutase and
472 1×10^4 cells/cm^2 or 1.5×10^4 cells/cm^2 were seeded on a 6-well plate pre-coated with Geltrex (Thermo
473 Fisher Scientific A1413302) directly into N2B27 medium supplemented with 10 µM ROCKi (day 0).
474 From day 1, cells were cultivated in N2B27 without ROCKi. For the additional conditions, the N2B27

475 was supplemented with 2 μM XAV939, 12 ng/mL FGF2 (in-house or PeproTech 100-18B) and/or 10
476 ng/mL Activin A (PeproTech 120-14E) or replaced with E8 or mTeSR.

477 Conversion of human naive PSCs into trophectoderm/TSCs

478 Naive hiPSCs HPD06 and HPD03 stably cultured on MEFs or serum coating were pre-treated on MEF
479 with TS medium for 24h. Cells were dissociated with TrypLE, and 5×10^4 cells/cm^2 were seeded on a
480 6-well plate pre-coated with 5 μg/mL Collagen IV and further cultured in TS medium (DMEM/F12
481 supplemented with 0.1 mM 2-mercaptoethanol, 0.2% FBS, 0.3%, Bovine serum albumin (BSA, Gibco
482 15260-037), 1% ITS-X (Gibco 51500), 1.5 μg/ml L-ascorbic acid (Merck Sigma Aldrich A4544), 50
483 ng/ml EGF (Qkine Qk011), 2 μM CHIR99021 (Axon Medchem 1386), 0.5 μM A83-01 (Axon
484 Medchem 1421), 1 μM SB431542 (Axon Medchem 1661), 0.8 mM VPA [HDACi, Merck Sigma
485 Aldrich P4543], and 5 μM ROCKi). Cells were cultured in 5% CO_2 and 5% O_2 changing medium every
486 2 days and were passaged upon 80% confluency at a 1:6 to 1:8 ratio.
487 Naive SIG-1 hiPSCs to trophoblast differentiation was done as previously published[39], using the
488 following previously described protocols for hTSCs[34–36,70]. Cells were cultured on MEFs or serum
489 coating until subconfluency and dissociated in single-cell using TryplE for 5 min at 37°C in PXGL
490 supplemented with 10 mM Y-27632 (Tocris, 1254). At day 2 of culture, cells were washed with PBS
491 (Gibco, 10010-015), and the media was switched from PXGL to ASECRiAV medium[87] consisting of
492 DMEM/F12 (Gibco, 31330038) supplemented with 0.3% BSA (Sigma A3059), 0.2% FBS (Gibco
493 10270-106), 1% Penicillin-streptomycin (Gibco 15140-122), 1% insulin-transferrin-selenium-
494 ethanolamine-X 100 supplement (Gibco 51500056), 1.5 mg/mL L-ascorbic acid (Sigma A8960), 0.5
495 mM A83-01 (Peprotech 9094360), 1 mM SB431542 (Axon Medchem 1661), 50 ng/ml hEGF (Miltenyi
496 Biotec 130-097-750), 2uM CHIR99021 (Axon Medchem 1386), 0.8 mM Valproic acid (Sigma
497 V0033000), 0.1 mM b-mercapto-EtOH (Gibco 31350- 010) and 5 mM Y-27632 (Tocris 1254). The
498 medium was changed every day and supplemented with 5 mM Y-27632. From passage 1 onwards
499 hTSCs were cultured and maintained on 1.5 mg/mL iMatrix-silk-E8-Laminin overnight coated tissue
500 culture treated plates in hypoxia conditions 5% O2 and 5% CO2 at 37°C and passaged every 5 days at
501 1:3 splitting ratio. hTSCs used in all experiments were cultured and maintained in ASECRiAV until
502 day 26 of conversion.
503 Naive SIG-1 hiPSCs differentiation to trophectoderm was performed as previously described[88]. Briefly,
504 cells were dissociated in single cells using Accutase at 37°C for 6 min, followed by gentle mechanical
505 dissociation. Single cells were counted and viability was assessed via trypan blue staining using
506 ThermoFisher Countess II and 3×10^4 live cells/cm^2 were plated onto iMatrix Silk laminin 511-coated
507 plate (Amsbio AMS.892 012) in nTE1 media (N2B27 supplemented with 2 μM A83-01 [Merck Sigma
508 Aldrich SML0788], 2 μM PD0325901 [Axon Medchem 1408], 10 ng/ml BMP4 [R&D Systems 314-
509 BP] and 10 μM Y-27632 [Tocris 1254]). After 24h, cells were washed with PBS and media switched

510 to nTE2 for 48h and refreshed daily (N2B27 supplemented with 2 μM A83-01, 2 μM PD0325901 and
511 1 μg/ml JAKi1 [Merck Sigma Aldrich 420099]). Cells were fixed on day 3.

512 Culture of BAP-treated primed pluripotent stem cells

513 MEFs were fed with DMEM/Ham's F-12 medium containing 0.1 mM 2-mercaptoethanol, 1% Insulin-
514 Transferrin-Selenium-Ethanolamine (ITS-X; Gibco 51500056), 1% non-essential amino acids (NEAA;
515 Gibco 11140050), 2 mM L-glutamine, and 20% KnockOut™ Serum Replacement (KSR; Gibco
516 10828028) for 24 h. The supernatant was collected and used as MEF-conditioned medium. KiPS were
517 dissociated into single cells with TrypLE. The cells were cultured on pre-coated plates with 0.5%
518 growth factor-reduced Matrigel at a density of 2×10^4 cells/cm^2 with MEF-conditioned medium
519 supplemented with 10 ng/ml BMP4 (Peprotech 120-05ET), 1 μM A83-01, 0.1 μM PD173074 (Axon
520 Medchem 1673), and 10 μM ROCKi, as described previously[36]. The medium was changed daily.

521 Spontaneous differentiation with embryoid bodies

522 Capacitated hiPSCs HPD06 from stable cultures on MEFs or serum coating were single-cell dissociated
523 with TrypLE and seeded at 1.5×10^4 cells in v-bottom 96-well plates (Greiner, M9686) pre-treated with
524 anti-adherence AggreWell™ Rinsing Solution (STEMCELL Technologies 7010) in E8 medium with
525 10 μM ROCKi (day 0). From day 1, aggregates were cultivated in spontaneous differentiation medium
526 (DMEM/F12 with 20% FBS, 2 mM L-glutamine, 1% NEAA and 0.1 mM 2-mercaptoethanol). Half of
527 the medium was changed every 2 days.

528 Blastoid formation

529 Blastoid experiments from naive H9 hESCs were performed according to Kagawa *et al*[41], with minor
530 modifications. Briefly, H9 naive hESCs were collected by incubation for 3 min with Accutase (Merck
531 Sigma Aldrich A6964). Single cells were plated at a density of 98-102 cells per micro-well of a 24-well
532 AggreWell™400 plate in N2B27 supplemented with 10 μM Y27632 (Axon Medchem 1683) to
533 aggregate for 3h. Subsequently, half medium was changed with 2x PALLY consisting of N2B27
534 supplemented with 1 μM PD0325901 (Axon Medchem 1408), 1 μM A83-01 (Axon Medchem 1421),
535 10 ng/mL hLIF (Qkine Qk036), 1 μM oleoyl-L-α-lysophosphatidic acid sodium salt (LPA, Merck
536 Sigma Aldrich L7260) and Y27632. 24 hours later, half-medium was changed with 1x PALLY. After
537 48h of PALLY culture, blastoids were maintained for 56 hours in LY medium consisting of N2B27
538 supplemented with LPA and Y27632. Blastoids from H9 naive hESCs were processed for single-cell
539 RNA sequencing at day 5.
540 Blastoid experiments from naive KOLF2.1J and SCTi003-A hiPSCs were performed according to
541 Kagawa et al.[41], with minor modifications. Naive KOLF2.1J and SCTi003-A hiPSCs were collected by
542 incubation with Accutase for 5 min. In the presence of MEFs, cells were incubated for 70 minutes on

543 0.1% gelatin-coated plates after which the non-attached hiPSCs were collected. Single cells were plated
544 at a density of 20.000 cells per well of a 96-well plate comprising microwells of 200 µm diameter, made
545 as previously described[89]. Cells were cultured in N2B27 supplemented with 0.3% BSA (Sigma Aldrich
546 A7979), 1µM PD0325901 (MedChem Express HY-10254), 1µM A83-01 (MedChem Express HY-
547 10432), 10ng/ml hLIF (in house), 1 µM LPA (Peprotech 2256236) and 1:1000 CEPT cocktail (Thermo
548 Fisher A56799). After 24 hours the medium was changed to N2B27 supplemented with 1 µM
549 PD0325901, 1 µM A83-01, 10 ng/ml LIF and 1 µM LPA for 48 hours with daily medium changes.
550 Blastoids were maintained for an additional 48 hours in N2B27 medium supplemented with 1 µM LPA.
551 Blastoid experiments from naive HNES1 hESCs were performed as previously described[41] using
552 AggreWells™400 (STEMCELL Technologies 34415). Briefly, naive HNES1 hESCs were treated with
553 Accutase at 37°C for 6 min, followed by gentle mechanical dissociation. Cell pellet was resuspended
554 in Aggregation medium composed of N2B27 with 0.3% BSA (Merck Sigma Aldrich A7979) and 10
555 µM Y-27632. Single cells were counted and viability assessed via trypan blue staining using
556 ThermoFisher Countess II and $1.0/1.2\times10^5$ live cells/well (~80/100 cells/µwell) were seeded into
557 AggreWells™400 and grown in a hypoxic chamber. AggreWells™400 were treated with an anti-
558 adherent solution (STEMCELL Technologies 07010) and washed 3 times (2x N2B27 and 1x
559 aggregation medium) before cell plating (day -1). The cells were allowed to form aggregates inside the
560 microwell for 24 hours. On day 0, the aggregation medium was replaced with PALLY medium: N2B27
561 with 0.3% BSA, 1 µM PD0325901, 1 µM A83-01 (Merck Sigma Aldrich SML0788), 0.5 µM LPA
562 (Tocris 3854), 10 ng/ml hLIF and 10 µM Y-27632. PALLY medium was refreshed on day 1. After 48
563 h (day 2) PALLY medium was replaced with N2B27 containing 0.3% BSA, 0.5 µM LPA and 10 µM
564 Y-27632 (LY medium). LY medium was refreshed on day 3, and blastoids fully formed on day 4.

565 Proliferation assay and AP staining

566 Cell proliferation was assessed by plating 5×10^4 cells/cm^2 in a 6-well plate. Cells were single-cell
567 dissociated with TrypLE, counted and re-plated every 3 days.
568 For AP staining, cells were fixed with a citrate–acetone–formaldehyde solution and stained using the
569 Alkaline Phosphatase kit (Merck Sigma Aldrich 86R-1KT). Plates were scanned using a Nikon Scanner
570 and scored with the Analyse Particles plugin of the software Fiji (from ImageJ) 1.0 (pixels 5-500,
571 circularity 0.5-1).

572 Gene expression analysis by quantitative PCR with reverse transcription

573 Total RNA from naive hiPSCs HPD06 and HPD03 was isolated using Total RNA Purification Kit
574 (Norgen Biotek 37500), and complementary DNA (cDNA) was made from 500 ng using M-MLV
575 Reverse Transcriptase (Invitrogen 28025-013) and dN6 primers. Data were acquired with the Applied
576 Biosystems QuantStudio™ 6&7 Flex Software 1.3.

577 Total RNA from naive hESCs H9 and Shef6 was isolated with the ExtractMe kit (Blirt EM15) following
578 the manufacturer's instructions, and cDNA was made from 100 ng using the SensiFAST cDNA
579 Synthesis Kit (Bioline BIO-65054). Real-time PCR was performed on the CFX384 Touch real-time
580 PCR detection system (Bio-Rad).
581 SYBR Green Master mix (Bioline BIO-94020) was used for real-time qPCR and primers are listed in
582 Supplementary Table 1. Three technical replicates were carried out for each biological replicate of all
583 RT-qPCR analyses and *β-ACTIN* or *GAPDH* were used as endogenous controls to normalise expression.

584 Immunofluorescence

585 Immunofluorescence analysis of naive hiPSCs HPD06 and HPD03 was performed on 1% Matrigel-
586 coated glass coverslip in wells. Cells were fixed in 4% Formaldehyde (Merck Sigma Aldrich 78775) in
587 PBS for 10 min at room temperature, washed in PBS, and permeabilised and blocked in PBS with 0.3%
588 Triton X-100 (PBST) and 5% of horse serum (ThermoFisher 16050-122) for 1 hour at room
589 temperature. Cells were incubated overnight at 4°C with primary antibodies in PBST with 3% horse
590 serum. After washing with PBS, cells were incubated with secondary antibodies (Alexa, Life
591 Technologies) for 45 min at room temperature. Nuclei were stained using Fluoroshield™ with DAPI
592 (Merck Sigma Aldrich F6057). Images were acquired with a Zeiss LSN700 confocal microscope using
593 ZEN 2012 software. Images were processed using the software Fiji (from ImageJ) 1.0. Fluorescence
594 intensity was quantified using Cell Profiler software (v4.2.1). DAPI staining was used to identify
595 individual nuclei of cells. At least 700 nuclei from five randomly selected fields from two independent
596 experiments were analysed for each condition. Single-cell measured mean intensity values were
597 considered for downstream data analysis.
598 For immunofluorescence analysis of naive H9 hESCs and Shef6 hiPSCs from Leeb's group, cells were
599 plated onto μ-Slide 8 Well Glass Bottom Chamber Slides (Ibidi 80827) with MEFs, or onto slides coated
600 with serum or Geltrex. Cells were fixed in 4% Formaldehyde in PBS for 20 min at room temperature,
601 washed in PBS, and permeabilised and blocked in PBS with 0.5 % Triton X-100 (PBST) and 5% BSA
602 for 30 min at room temperature. Cells were incubated overnight at 4°C with primary antibodies in PBST
603 with 5% BSA. After washing with PBS, cells were incubated with secondary antibodies (Alexa, Life
604 Technologies) for 1h at room temperature. After washing with PBS, the nuclei were stained with 20
605 ng/mL DAPI in PBS (Invitrogen D1306) for 5 min in the dark at room temperature. Samples were
606 mounted using Vectashield with DAPI (Vector Laboratories VECH-1200). Images were acquired with
607 an Axio Observer Z1 microscope and processed using the software Fiji (from ImageJ) 1.0.
608 Immunofluorescence staining protocol was performed in naive H9 hESCs from Pasque's group and
609 SIG-1 hiPSC as previously published[39,90]. Cells were grown on 0.1% gelatinised 18 mm round
610 coverslips on MEFs or serum coating. Cells were fixed in 4% paraformaldehyde-PBS for 10 min at
611 room temperature in the dark and permeabilised with 0.5% Triton X-100 in PBS for 5 min and washed

612 twice with 0.2% Tween 20 in PBS (PBST) for 5 min each before proceeding to the staining. Primary
613 and secondary antibodies were diluted in a blocking buffer containing mainly 2% Tween-PBS with 5%
614 normal donkey serum and 0.2% fish skin gelatin. Cells on coverslips were incubated overnight at 4°C
615 with the specific primary antibodies in blocking solutions (1:50 dilution for NANOG, 1:300 dilution
616 for KLF17), then washed three times with PBST for 5 min. After washing, the samples were incubated
617 with secondary antibodies diluted in blocking buffer for 1 hour in the dark at room temperature. The
618 samples were then washed with PBST three times for 5 min each and afterwards washed with 0.002%
619 DAPI (Sigma-Aldrich D9542) solution in PBST. The coverslips were mounted in Prolong Gold reagent
620 with DAPI after a final wash in PBST. Naive hPSCs immunofluorescence images were taken in a Nikon
621 TiE A1R inverted microscope and were processed using the software Fiji (from ImageJ) 1.0.
622 Blastoids from naive H9 hESCs were fixed with 4% paraformaldehyde for 20 min at room temperature.
623 Subsequently, the samples were washed for 3 times 10 minutes with PBST (PBS containing 0.1%
624 Tween20) supplemented with BSA (0.3%). The samples were then permeabilised for 20 min using 0.2%
625 Triton X-100 in PBS and afterwards blocked using a blocking buffer containing 0.1% Tween20, 1%
626 BSA and 10% normal donkey serum in PBS for at least 3 hours. The samples were then incubated
627 overnight at 4°C with primary antibodies diluted in blocking buffer. The next day, samples were washed
628 with PBST at least three times for 10 min each. After washing, the samples were incubated with
629 secondary antibodies diluted in blocking buffer for 3 hours in the dark at room temperature. The samples
630 were then washed with PBST three times for 10 min each and afterwards mounted using PBS. Image
631 acquisition was performed using a Leica Stellaris 5 fluorescence confocal microscope and were
632 processed using the software Fiji (from ImageJ) 1.0.
633 Blastoids from naive KOLF2.1J and SCTi003-A hiPSCs were fixed with 4% PFA for 30 min at room
634 temperature and rinsed three times with PBS. Samples were permeabilised and blocked using 0.3%
635 Triton X-100 and 10% normal donkey serum in PBS for at least 60 min and incubated overnight at
636 room temperature with primary antibodies diluted in fresh blocking/permeabilisation buffer. The
637 following day samples were washed with PBS containing 0.1% Triton X-100 (PBST) at least three
638 times for 10 min each. Samples were then incubated in Alexa Fluor-tagged secondary antibodies
639 (Abcam or Thermofisher Scientific) diluted in PBST for at least 30 min in the dark at room temperature
640 and washed three times with PBST for 10 min each. Images were captured using an Olympus IX83
641 confocal microscope. Each image consisted of 30 optical sections, with an average thickness of
642 approximately 3–5µm per section. Images were processed using the software Fiji (from ImageJ) 1.0.
643 Blastoids from naive HNES1 hESCs were fixed with 4% PFA for 30 min at room temperature and
644 rinsed three times with PBS. About 10-20 structures per condition were then moved to Thermo
645 Scientific™ Nunc™ MiniTrays with Nunclon™ Delta surface and permeabilised for 30 min at RT using
646 PBS/0.3% Triton X-100 (Merck Sigma Aldrich). Cells were blocked for 4-6h at RT with blocking
647 solution (PBS 0.3% Triton X-100 with 10% Normal Donkey Serum [Merck Sigma Aldrich S30]).
648 Primary antibodies (listed in Supplementary Table 2) were diluted in blocking solution and incubated

649 overnight at 4°C in a humidified chamber. Cells were washed three times with PBS 0.1% Triton X-100,
650 and stained with secondary antibodies for 1h at RT in a humidified chamber. Cells were washed three
651 times with PBS 0.1% Triton X-100, and stained with DAPI for 15 min at RT during the second wash
652 (0.1 µg/ml DAPI in PBS 0.1% Triton X-100). Finally, blastoids were moved into IBIDI µ-Slide 15 Well
653 3D Glass Bottom (81507) and imaged using a C2 or TiE A1R confocal microscope (Nikon). Images
654 were processed using the software Fiji (from ImageJ) 1.0, Z-stacks were shown as Max Intensity
655 projections and denoised using the "despeckle" tool equally on all images.
656 All used primary antibodies are listed in Supplementary Table 2.

657 Flow cytometry

658 For flow cytometry analysis, naive and differentiating Shef6 hESCs and primed hPSCs were detached
659 using Accutase and resuspended in DMEM supplemented with 0.5% BSA. For surface marker staining
660 the cells were washed 1x in FACS buffer (1x PBS and 1% BSA), stained with APC-conjugated anti-
661 human SUSD2 antibody (BioLegend 327408) diluted 1:100 in FACS buffer for 30 min on ice in the
662 dark and washed again 1x with FACS buffer. For live/dead discrimination 5 µg/mL DAPI (Invitrogen
663 D1306) was used. Antibody signal levels were measured using the ZE5 (Bio-Rad) and then analysed
664 with the FlowJo software (v10.10, BD Bioscience).
665 Nave H9 hESCs and SIG-1 hiPSCs were first stained for viability in 1:300 Live/Death Zombie Aqua
666 UV in PBS. Fluorophore conjugated antibody was diluted at a ratio of 1:50 in fluorescence-activated
667 cell sorting (FACS) buffer with PE-conjugated anti-human SUSD2 (Biolegend, 327406), for 20 minutes
668 at room temperature, then washed with FACS buffer, and fixed in 4% paraformaldehyde. Cells were
669 passed through a 40 µm cell strainer (Corning 352340). The fluorescence intensity of 20,000 cells was
670 recorded on a flow cytometer (Symphony A5, BD Biosciences) and analyzed using FlowJo software
671 (v10.10, BD Bioscience). Single-stained controls were used for compensation and gating in the flow
672 cytometer. Only lived cells were used for data analysis. The frequency of the parent population has been
673 used to plot the SUSD2-positive cells.

674 Proteomics

675 Samples were processed using the PreOmics iST sample preparation kit (PreOmics P.O.00027). LC-
676 MS/MS analysis consisted of a NanoLC 1200 coupled via a nano-electrospray ionization source to the
677 quadrupole-based Q Exactive HF benchtop mass spectrometer[91]. For the chromatographic separation, a
678 binary buffer system consisting of solution A: 0.1% formic acid and B: 80% acetonitrile, 0.1% formic
679 acid was used. Peptides were separated according to their hydrophobicity on an analytical column (75
680 µm) in-house packed with C18-AQ 1.9 µm C18 resin with a gradient of 7–32% solvent B in 45 min,
681 32–45% B in 5 min, 45–95% B in 3 min, 95–5% B in 5 min at a flow rate of 300 nl/min. MS data
682 acquisition was performed in DIA (Data Independent Acquisition) mode using 32 variable windows

683 covering a mass range of 300–1650 m/z. The resolution was set to 60’000 for MS1 and 30’000 for MS2.
684 The AGC was 3e6 in both MS1 and MS2, with a maximum injection time of 60 ms in MS1 and 54 ms
685 in MS2. NCE was set to 25%, 27.5%, 30%. All acquired raw files were processed using Spectronaut
686 software (17.0). For protein assignment, spectra were correlated with the Rattus Norvegicus/Bos Taurus
687 database (v. 2023). Searches were performed with tryptic specifications and default settings for mass
688 tolerances for both MS and MS/MS spectra.
689 The other parameters were set as follows. Fixed modifications: Carbamidomethyl (C); variable
690 modifications: Oxidation, Acetyl (N-term); digestion: Trypsin, Lys-C; min. peptide length = 7Da; max.
691 peptide mass = 470Da; false discovery rate for proteins and peptide-spectrum = 1%. Perseus software
692 (1.6.2.3) was used to logarithmise, group and filter the protein abundance. The obtained list of proteins
693 was analysed using the Matrisome AnalyseR tool
694 (https://sites.google.com/uic.edu/matrisome/tools/matrisome-analyzer[62]) from The Matrisome Project.

695 Exome sequencing

696 NEGEDIA S.r.l. performed the Exome Sequencing service. Genomic DNA was extracted with a
697 paramagnetic beads technology using the Negedia DNA extraction service, quantified using the Qubit
698 4.0 fluorimetric Assay (Thermo Fisher Scientific) and sample integrity, based on the DIN (DNA
699 integrity number), was assessed using a Genomic DNA ScreenTape assay on TapeStation 4200 (Agilent
700 Technologies). Libraries were prepared from 100 ng of total DNA using the NEGEDIA Exome
701 sequencing service which included library preparation, target enrichment using Agilent V8 probe set,
702 quality assessment with FastQC v0.11.9 (https://www.bioinformatics.babraham.ac.uk/projects/fastqc/)
703 and sequencing on a NovaSeq 6000 system using a paired-end, 2x150 cycle strategy (Illumina Inc.).
704 The raw data were analysed by NEGEDIA Exome pipeline (v1.0) which involves, alignment to the
705 reference genome (hg38, GCA_000001405.15), removal of duplicate reads and variant calling with
706 Sentieon 202308[92]. Variants were annotated by the Ensembl Variant Effect Predictor (VEP) tool3 (v.
707 104)[93]. Annotated variants were selected based on: impact on protein High/Moderate, base depth ≧30,
708 alternate depth ≧5 and alt/base depth ≧5%. Selected variants were finally classified with Varsome
709 Clinical (https://eu.clinical.varsome.com/).

710 Bulk RNA sequencing and analysis

711 Total RNA from HPD06 and HPD03 naive hiPSCs was isolated as previously described, and Quant
712 Seq 3' mRNA-seq Library Prep kit (Lexogen) was used for library construction. Before sequencing
713 library quantification was performed by fluorometer (Qubit) and bioanalyzer (Agilent). Sequencing was
714 performed on NextSeq500 ILLUMINA instruments to produce 5 million reads (75bp SE) for each
715 sample. Transcript quantification was performed from raw reads using Salmon (v1.6.0)[94] on transcripts
716 defined in Ensembl 106. Gene expression levels were estimated with tximport R package (v1.26.1)[95].

717 Batch correction was performed using the ComBat_seq function from the sva R package (v3.50.0;
718 https://bioconductor.org/packages/release/bioc/html/sva.html). Batches have been defined following
719 library preparation: batch 1 for full-length libraries and batch 2 for Quant Seq 3′ mRNA-seq Library
720 Prep kit. CPM on batch corrected counts were computed using the CPM function of the edgeR package
721 (v4.0.12[96]). PCA was performed using the svd r function on log-transformed CPM. All plots except the
722 heatmaps have been done using ggplot2 v3.5.1 (https://ggplot2.tidyverse.org/authors.html#citation).
723 Heatmap was done using the pheatmap R package (v1.0.12). All analyses were performed using R
724 v4.3.2.
725 Imprinted genes analysis of HPD00 primed and HPD06 and HPD03 naive hiPSCs have been performed
726 by submitting the .fastq raw files to BrewerIX (https://brewerix.bio.unipd.it)[45], implementing the
727 complete pipeline and evaluating the significant genes.
728 Total RNA from naive hESCs Shef6 was isolated as previously described. Library preparation with the
729 Quant Seq 3' mRNA-seq Library Prep kit (Lexogen) and sequencing with the Illumina NextSeq2000
730 P3 platform was carried out at the VBCF NGS facility, producing 5-10 million reads (50 bp SE). For
731 analysis of the fastq files the Nextflow 23.04.1.5866/nf-core/rnaseq v3.10.1 pipeline was used. This
732 included quality control with fastQC (v0.11.9), pseudo-alignment to the human reference genome hg38
733 with Salmon (v1.9.0) and alignment with STAR (v2.7.10a). Gene expression levels were estimated with
734 the tximport R package (v1.26.1)[95]. DESeq2 (v1.38.3) was used for further analysis including
735 differential expression analyses. For comparison with already published data[68], the batch correction was
736 performed using the ComBat_seq function from the sva R package (v3.46.0). For PCAs, counts were
737 transformed with the regularised log transformation (rlog) function (for own time course) or the
738 variance-stabilising transformation (vst) function (integration with Rostovskaya data) from DESeq2.
739 All plots except heatmap have been done using ggplot2 v3.5.1. Heatmaps were done with the pheatmap
740 R package (v1.0.12) using row-wise z-transformed DESeq2-normalized counts. All analyses were
741 performed using R v4.3.2.

742 Single-cell RNA sequencing, analysis and comparison with bulk RNA 743 sequencing

744 For the analyses of the pluripotency exit, the human embryogenesis reference dataset[69] was derived by
745 the integration of six published human datasets[20,40,75–78] covering developmental stages from the zygote
746 to the gastrula was kindly provided by the Petropoulos lab. Analysis was performed using Seurat v5.1.0
747 and the data was subset for embryonic cells covering E5-E14. For the PCA, pseudobulk data was
748 generated with Seurat's AggregateExpression function and integrated with the bulk RNA-seq data using
749 DESeq2 v1.38.3. Batch correction for the datasets was performed using the ComBat_seq function
750 before applying variance stabilising transformation with the vst function from DESeq2. Heatmaps and

boxplots were generated using the Shiny app (http://petropoulos-lanner-labs.clintec.ki.se) from the reference dataset[69].

For blastoids validation blastoids were dissociated into a single cell suspension by incubation with a mixture of TrypLE™ (Thermo Fisher Scientific A1217701) and Accutase (Merck Sigma Aldrich A6964). The sample was incubated with 0.5 µg of unique hashtag antibody for 20 min on ice. TotalSeq hashtag antibodies (Biolegend) were used to multiplex the samples[97]. The sample was sorted on a BD FACSymphony S6 (BD Biosciences) and then loaded onto a Chromium Next GEM chip (10x Genomics). Further steps of library preparation were performed according to the Chromium Next GEM Single Cell 3' v3.1 user guide with the addition of the hashtag library for demultiplexing. Combined libraries were sequenced using the NextSeq2000 P2-100 kit (Illumina) with Paired-end sequencing. Initial processing of scRNA-seq data was performed using Cell Ranger (v 6.1.2, 10X Genomics). Dual-indexed RNA and single-indexed hashtag oligo (HTO) libraries were processed in separate instances of cellranger mkfastq, using Illumina's bcl2fastq (v2.20.0.422). FASTQ files were aligned to the human reference genome (GRCh38, v 2020-A as provided by 10x Genomics) with cellranger multi (expect-cells 16500, min-assignment-confidence 0.9), assigning 4251 cells to the sample of interest. The resulting filtered feature-barcode matrix was loaded into Seurat (v 4.3.0)[98], excluding features that were detected in less than three cells. Next, RNA data was normalised with the default LogNormalize method, and the HTO assay was normalised with centered log-ratio (CLR) transformation. Based on QC plots, cells with more than 15% mitochondrial counts or less than 7000 UMIs (nCount_RNA) were removed, retaining 3260 high-quality cells. These were subjected to standard Seurat processing using mostly default parameters unless indicated: FindVariableFeatures, ScaleData, RunPCA, RunUMAP (dims=1:15), FindNeighbors (dims=1:15), FindClusters (resolution=0.5). To characterise the cells' cycling status, the function CellCycleScoring was run using the built-in lists of S and G2M phase markers (cc.genes.updated.2019) derived from[99]. Cells separated by cell cycle phase on the UMAP and this source of heterogeneity was then regressed out using ScaleData (vars.to.regress = c("S.Score", "G2M.Score"), features = rownames(object)), followed by RunPCA, RunUMAP(dims=1:15), FindNeighbors(dims=1:15), and FindClusters(resolution=0.5), resulting in 5 clusters. The raw counts of the quality-filtered matrix was uploaded to the Early Embryogenesis Projection Tool (v2.1.1) (https://petropoulos-lanner-labs.clintec.ki.se/shinys/app/ShinyEmbryoProjP, accessed on 2024-09-26) to project the cells on an integrated reference UMAP of human embryo development and get annotation of predicted cell identities[69].

Statistics and reproducibility

For each dataset, sample size *n* refers to the number of biological or technical replicates, shown as dots and stated in the figure legends. All error bars indicate the standard error of the mean (SEM). All RT-qPCR experiments were performed in three technical replicates.

Ethics statement

Our research complies with all relevant ethical regulations including ISSCR guidelines. HPD06 and HPD03 naive hiPSCs used in G.M.'s Laboratory were checked by the European ethics committee and registered in the human pluripotent stem cells registry (link: https://hpscreg.eu/ cell-line/UNIPDi004-B). Experiments with hPSCs and blastoids in J.J.Z's Laboratory were approved by the Scientific Ethics Committee for Hovedstaden (H-21043866/94634 and H-24048289). Shef6 line use is with the agreement of the Steering Committee of the UK Stem Cell Bank (SCSC16-09). The WiCell line H9 (WA09) was used under the agreements 23-W0460 (JJZ) and 21-W0002 (ML). Work with human embryonic and induced pluripotent stem cells including blastoids in V.P. Laboratory was approved by the UZ/KU Leuven ethics committee (S64962, S66595 and S68981). Work with mouse embryonic fibroblast was approved by the UZ/KU Leuven ethics committee (P170/2019). The Austrian Academy of Sciences (the local ethical body) has given N.R.'s Laboratory a license to perform blastoid experiments, following expert legal advice that concluded these are not in conflict with Austrian laws. This license is in the shape of a statement of the Commission for Science Ethics of the Austrian Academy of Sciences concerning the project 'Modeling human early development using stem cells'. There is no approval number on that document. This license conforms with the ethical standards suggested by the International Society for Stem Cell Research (ISSCR). This work did not exceed a developmental stage normally associated with 14 consecutive days in culture after fertilization nor did it entail any implantation *in vivo*.

Inclusion & ethics statement

All collaborators of this study have fulfilled the criteria for authorship required by Nature Portfolio journals and have been included as authors, as their participation was essential for the design and implementation of the study. Roles and responsibilities were agreed among collaborators ahead of the research. This research was not severely restricted or prohibited in the setting of the researchers and does not result in stigmatisation, incrimination, discrimination or personal risk to participants.

Data availability

Bulk and single-cell RNA-seq data for this study have been deposited in the Gene Expression Omnibus (GEO) database under the accession code GSE284370. We also included available RNA-Seq data for naive and primed hPSCs, hTSCs and fibroblasts from GSE110377[30], GSE63577[100], GSE93226[101], GSE75868[43], GSE184562[72], GSE138688[34], GSE178162[102], GSE135695[103], PRJNA397941[27], GSE133630[104], GSE73211[105], PRJEB7132[24], PRJEB12748[26]; for capacitation from GSE123055[68]; for embryonic development from the human embryogenesis reference dataset[69], comprehensive of GSE36552[20], E-MTAB-3929[75], GSE136447[76], E-MTAB-9388[78], GSE171820[40], PRJEB30442[77].

Proteomics data have been deposited in the PRIDE Proteomics database under the accession code PXD059820.

Acknowledgements

We thank the KU Leuven FACS Core team for supporting flow cytometry experiments, Alejandra Purcell from Gorgas Institute in FACS analysis, and the VIB BioImaging Core Leuven for their contribution to imaging performed in V.P. lab. We thank the Vienna Biocenter Core Facilities (VBCF) for support in NGS analysis. J.J.Z's team thanks Antar Drews and Sandra Bages Arnal for their input, the reNEW platforms for technical expertise, support and use of equipment in particular: H. Wollmann, M. Michaut, J. Bulkescher, G. Dela Cruz and A. Kalvisa.

G.M.'s Laboratory is supported by grants from: Giovanni Armenise–Harvard Foundation, Telethon Foundation (GJC21157), European Research Council Starting Grant (716910 - MetEpiStem), Italian national project 'PRIN 2022' (2022RA8E3T) and La Caixa Foundation (LCF/PR/HR24/52440015). G.R. is supported by a HORIZON MSCA Postdoctoral Fellowship (101108873 - PLURImet). M.L.'s Laboratory is supported by grants from the Austrian Science Fund (FWF; P35637, I5958). M.O. is a member of the FWF-funded doctoral programme 'Signalling Molecules in Cellular Homeostasis' (SMICH; W1261), and M.L. is a faculty member and speaker of SMICH and a 'Wiener Wissenschafts-Forschungs- und Technologiefonds (WWTF)' Vienna Research Group Leader (VRG14-006). V.P.'s Laboratory is supported by the Research Foundation-Flanders (FWO grants G0C9320N and G0B4420N to V.P.), KU Leuven Research Fund (C1 grant C14/21/119 to V.P.), and Pandarome project 40007487 (G0I7822N) (funded by the FWO and F.R.S.-FNRS) under the Excellence of Science (EOS) program. M.A.S. is supported by Gorgas Memorial Institute for Health Studies and Fundación Sus Buenos Vecinos in Panama. S.S.F.A.v.K. (11I1523N) and T.X.A.P. (11N3122N) are supported by FWO PhD fellowships. J.J.Z.'s Laboratory is supported by grants from: Novo Nordisk Fonden (NNF21CC0073729), Lundbeckfonden (R345-2020-14979), Danmarks Frie Forskningsfond (0169-00031B) and the European Research Council Starting Grant (101077271 - ChroMeta). N.R.'s Laboratory is supported by the European Research Council (ERC) under the European Union's Horizon 2020 research and innovation programme (ERC-Co grant agreement no. 101002317, "BLASTOID: a discovery platform for early human embryogenesis").

D.C. is supported by Fondazione Telethon Core Grant, Italian Ministry of Health (Piano Operativo Salute Traiettoria 3, T3-AN-09, "Genomed"; Ricerca Finalizzata 2021, "genOMICA"; MCNT2 2023, "EUCARDIS"), Italian Ministry of University and Research and European Union (Next Generation EU - MUR-PRIN-2022, Project PNC 0000001 D3 4 Health). P.G. is supported by Fondazione Telethon Core Grant, AIRC (MFAG 2020), PNRR (PNRR-MR1-2022-12376821), PRIN-2022-PNRR (P2022JLNZ7), PRIN (20224FL9T5). P.M. is supported by the Italian national project 'PRIN 2022' (2022LJZRBY).

Author contributions

G.R. performed experiments and analysed data (characterisation, embryonic and TSCs differentiation, bulk RNA-Seq, proteomics), supervised the study, prepared figures and wrote the manuscript; I.Z., performed experiments (characterisation) and edited the manuscript; A.D. performed experiments (characterisation); G.P. and N.M. performed experiments (characterisation, embryonic and TSC differentiation); P.M. analysed bulk RNA-Seq for the comparison with published datasets; C.C. and D.C. generated and analysed Exome-Seq data; P.G. performed proteomics experiments; G.M. conceived and supervised the study, secured funding and wrote the manuscript. M.O. performed experiments and analysed NGS data (embryonic differentiation), wrote the manuscript and prepared figures; M.L. supervised the study, secured funding and wrote the manuscript. A.O. and E.v.G. performed experiments (blastoids); M.A.S., S.S.F.A.v.K., T.X.A.P., and S.K. performed experiments (characterisation, TSC differentiation); N.R. and V.P. supervised the study, edited the manuscript and secured funding. I.S.B. performed experiments (blastoids), analysed the data, prepared figures and edited the manuscript; A.W. analysed and curated scRNAseq data; J.J.Z. supervised the study, secured funding, prepared figures and wrote the manuscript.

Disclosure and competing interests statement

Davide Cacchiarelli is founder, shareholder, and consultant of NEGEDIA S.r.l. Chiara Colantuono is an employee of NEGEDIA S.r.l.

References

1. Thomson, J. A. *et al.* Embryonic Stem Cell Lines Derived from Human Blastocysts. *Science* **282**, 1145–1147 (1998).
2. Evans, M. J. & Kaufman, M. H. Establishment in culture of pluripotential cells from mouse embryos. *Nature* **292**, 154–156 (1981).
3. Smith, A. G. *et al.* Inhibition of pluripotential embryonic stem cell differentiation by purified polypeptides. *Nature* **336**, 688–690 (1988).
4. Williams, R. L. *et al.* Myeloid leukaemia inhibitory factor maintains the developmental potential of embryonic stem cells. *Nature* **336**, 684–687 (1988).
5. Ying, Q.-L. *et al.* The ground state of embryonic stem cell self-renewal. *Nature* **453**, 519–523 (2008).
6. Martello, G. & Smith, A. The Nature of Embryonic Stem Cells. *Annu. Rev. Cell Dev. Biol.* **30**, 647–675 (2014).
7. Dunn, S.-J., Martello, G., Yordanov, B., Emmott, S. & Smith, A. G. Defining an essential transcription factor program for naïve pluripotency. *Science* **344**, 1156–1160 (2014).
8. Carbognin, E., Betto, R. M., Soriano, M. E., Smith, A. G. & Martello, G. Stat3 promotes mitochondrial transcription and oxidative respiration during maintenance and induction of naive pluripotency. *EMBO J.* **35**, 618–634 (2016).
9. Betto, R. M. *et al.* Metabolic control of DNA methylation in naive pluripotent cells. *Nat. Genet.* **53**, 215–229 (2021).
10. Takahashi, K. *et al.* Induction of Pluripotent Stem Cells from Adult Human Fibroblasts by Defined Factors. *Cell* **131**, 861–872 (2007).
11. Yu, J. *et al.* Induced Pluripotent Stem Cell Lines Derived from Human Somatic Cells. *Science* **318**, 1917–1920 (2007).
12. Hanna, J. *et al.* Human embryonic stem cells with biological and epigenetic characteristics similar to those of mouse ESCs. *Proc. Natl. Acad. Sci.* **107**, 9222–9227 (2010).
13. Ludwig, T. E. *et al.* Feeder-independent culture of human embryonic stem cells. *Nat. Methods* **3**, 637–646 (2006).
14. Braam, S. R. *et al.* Recombinant Vitronectin Is a Functionally Defined Substrate That Supports Human Embryonic Stem Cell Self-Renewal via αVβ5 Integrin. *Stem Cells* **26**, 2257–2265 (2008).
15. Chen, G. *et al.* Chemically defined conditions for human iPSC derivation and culture. *Nat. Methods* **8**, 424–429 (2011).
16. Brons, I. G. M. *et al.* Derivation of pluripotent epiblast stem cells from mammalian embryos. *Nature* **448**, 191–195 (2007).
17. Tesar, P. J. *et al.* New cell lines from mouse epiblast share defining features with human embryonic stem cells. *Nature* **448**, 196–199 (2007).
18. Huang, Y., Osorno, R., Tsakiridis, A. & Wilson, V. In Vivo Differentiation Potential of Epiblast Stem Cells Revealed by Chimeric Embryo Formation. *Cell Rep.* **2**, 1571–1578 (2012).
19. Nichols, J. & Smith, A. Naive and Primed Pluripotent States. *Cell Stem Cell* **4**, 487–492 (2009).
20. Yan, L. *et al.* Single-cell RNA-Seq profiling of human preimplantation embryos and embryonic stem cells. *Nat. Struct. Mol. Biol.* **20**, 1131–1139 (2013).
21. Buecker, C. *et al.* A murine-ES like state facilitates transgenesis and homologous recombination in human pluripotent stem cells. *Cell Stem Cell* **6**, 535 (2010).
22. Chan, Y.-S. *et al.* Induction of a Human Pluripotent State with Distinct Regulatory Circuitry that Resembles Preimplantation Epiblast. *Cell Stem Cell* **13**, 663–675 (2013).
23. Gafni, O. *et al.* Derivation of novel human ground state naive pluripotent stem cells. *Nature* **504**, 282–286 (2013).
24. Takashima, Y. *et al.* Resetting Transcription Factor Control Circuitry toward Ground-State Pluripotency in Human. *Cell* **158**, 1254–1269 (2014).
25. Theunissen, T. W. *et al.* Systematic Identification of Culture Conditions for Induction and Maintenance of Naive Human Pluripotency. *Cell Stem Cell* **15**, 471–487 (2014).
26. Guo, G. *et al.* Naive Pluripotent Stem Cells Derived Directly from Isolated Cells of the Human

929 Inner Cell Mass. *Stem Cell Rep.* **6**, 437–446 (2016).
930 27. Liu, X. *et al.* Comprehensive characterization of distinct states of human naive pluripotency
931 generated by reprogramming. *Nat. Methods* **14**, 1055–1062 (2017).
932 28. Kilens, S. *et al.* Parallel derivation of isogenic human primed and naive induced pluripotent
933 stem cells. *Nat. Commun.* **9**, 360 (2018).
934 29. Wang, Y. *et al.* Unique molecular events during reprogramming of human somatic cells to
935 induced pluripotent stem cells (iPSCs) at naïve state. *eLife* **7**, e29518 (2018).
936 30. Giulitti, S. *et al.* Direct generation of human naive induced pluripotent stem cells from somatic
937 cells in microfluidics. *Nat. Cell Biol.* **21**, 275–286 (2019).
938 31. Dutta, D. *et al.* Self-Renewal Versus Lineage Commitment of Embryonic Stem Cells: Protein
939 Kinase C Signaling Shifts the Balance. *Stem Cells* **29**, 618–628 (2011).
940 32. Bredenkamp, N. *et al.* Wnt Inhibition Facilitates RNA-Mediated Reprogramming of Human
941 Somatic Cells to Naive Pluripotency. *Stem Cell Rep.* **13**, 1083–1098 (2019).
942 33. Castel, G. *et al.* Induction of Human Trophoblast Stem Cells from Somatic Cells and Pluripotent
943 Stem Cells. *Cell Rep.* **33**, 108419 (2020).
944 34. Dong, C. *et al.* Derivation of trophoblast stem cells from naïve human pluripotent stem cells.
945 *eLife* **9**, e52504 (2020).
946 35. Guo, G. *et al.* Human naive epiblast cells possess unrestricted lineage potential. *Cell Stem Cell*
947 **28**, 1040-1056.e6 (2021).
948 36. Io, S. *et al.* Capturing human trophoblast development with naive pluripotent stem cells in vitro.
949 *Cell Stem Cell* **28**, 1023-1039.e13 (2021).
950 37. Linneberg-Agerholm, M. *et al.* Naïve human pluripotent stem cells respond to Wnt, Nodal and
951 LIF signalling to produce expandable naïve extra-embryonic endoderm. *Development* **146**,
952 dev180620 (2019).
953 38. Okubo, T. *et al.* Hypoblast from human pluripotent stem cells regulates epiblast development.
954 *Nature* **626**, 357–366 (2024).
955 39. Pham, T. X. A. *et al.* Modeling human extraembryonic mesoderm cells using naive pluripotent
956 stem cells. *Cell Stem Cell* **29**, 1346-1365.e10 (2022).
957 40. Yanagida, A. *et al.* Naive stem cell blastocyst model captures human embryo lineage
958 segregation. *Cell Stem Cell* **28**, 1016-1022.e4 (2021).
959 41. Kagawa, H. *et al.* Human blastoids model blastocyst development and implantation. *Nature* **601**,
960 600–605 (2022).
961 42. Yu, L. *et al.* Blastocyst-like structures generated from human pluripotent stem cells. *Nature* **591**,
962 620–626 (2021).
963 43. Theunissen, T. W. *et al.* Molecular Criteria for Defining the Naive Human Pluripotent State.
964 *Cell Stem Cell* **19**, 502–515 (2016).
965 44. Pastor, W. A. *et al.* Naïve human pluripotent cells feature a methylation landscape devoid of
966 blastocyst or germline memory. *Cell Stem Cell* **18**, 323–329 (2016).
967 45. Martini, P. *et al.* BrewerIX enables allelic expression analysis of imprinted and X-linked genes
968 from bulk and single-cell transcriptomes. *Commun. Biol.* **5**, 1–12 (2022).
969 46. Zhou, W. *et al.* HIF1α induced switch from bivalent to exclusively glycolytic metabolism during
970 ESC-to-EpiSC/hESC transition. *EMBO J.* **31**, 2103–2116 (2012).
971 47. Gu, W. *et al.* Glycolytic Metabolism Plays a Functional Role in Regulating Human Pluripotent
972 Stem Cell State. *Cell Stem Cell* **19**, 476–490 (2016).
973 48. Xie, C., Lin, G., Luo, K., Luo, S. & Lu, G. Newly expressed proteins of mouse embryonic
974 fibroblasts irradiated to be inactive. *Biochem. Biophys. Res. Commun.* **315**, 581–588 (2004).
975 49. Schnabel, L. V., Abratte, C. M., Schimenti, J. C., Southard, T. L. & Fortier, L. A. Genetic
976 background affects induced pluripotent stem cell generation. *Stem Cell Res. Ther.* **3**, 30 (2012).
977 50. Azizi, H., Ghasemi Hamidabadi, H. & Skutella, T. Differential Proliferation Effects after Short-
978 Term Cultivation of Mouse Spermatogonial Stem Cells on Different Feeder Layers. *Cell J.* **21**,
979 186–193 (2019).
980 51. Choupani, F. *et al.* Feeding role of mouse embryonic fibroblast cells is influenced by genetic
981 background, cell passage and day of isolation. *Zygote* **30**, 550–560 (2022).
982 52. Cesare, E. *et al.* 3D ECM-rich environment sustains the identity of naive human iPSCs. *Cell*
983 *Stem Cell* **29**, 1703-1717.e7 (2022).

53. Szczerbinska, I. *et al.* A Chemically Defined Feeder-free System for the Establishment and Maintenance of the Human Naive Pluripotent State. *Stem Cell Rep.* **13**, 612–626 (2019).
54. Puck, T. T., Cieciura, S. J. & Robinson, A. GENETICS OF SOMATIC MAMMALIAN CELLS : III. LONG-TERM CULTIVATION OF EUPLOID CELLS FROM HUMAN AND ANIMAL SUBJECTS. *J. Exp. Med.* **108**, 945–956 (1958).
55. Holmes, R. PREPARATION FROM HUMAN SERUM OF AN ALPHA-ONE PROTEIN WHICH INDUCES THE IMMEDIATE GROWTH OF UNADAPTED CELLS IN VITRO. *J. Cell Biol.* **32**, 297–308 (1967).
56. Hayman, E. G., Pierschbacher, M. D., Suzuki, S. & Ruoslahti, E. Vitronectin--a major cell attachment-promoting protein in fetal bovine serum. *Exp. Cell Res.* **160**, 245–258 (1985).
57. Hayman, E. G., Pierschbacher, M. D., Ohgren, Y. & Ruoslahti, E. Serum spreading factor (vitronectin) is present at the cell surface and in tissues. *Proc. Natl. Acad. Sci.* **80**, 4003–4007 (1983).
58. Hayman, E. G. & Ruoslahti, E. Distribution of fetal bovine serum fibronectin and endogenous rat cell fibronectin in extracellular matrix. *J. Cell Biol.* **83**, 255–259 (1979).
59. Murray, P. *et al.* The self-renewal of mouse embryonic stem cells is regulated by cell–substratum adhesion and cell spreading. *Int. J. Biochem. Cell Biol.* **45**, 2698 (2013).
60. Balbasi, E., Guven, G. & Terzi Cizmecioglu, N. Mouse Embryonic Stem Cell Culture in Serum-Containing or 2i Conditions. in *Embryonic Stem Cell Protocols* (ed. Turksen, K.) 275–294 (Springer US, New York, NY, 2022). doi:10.1007/7651_2021_438.
61. Vallier, L., Alexander, M. & Pedersen, R. A. Activin/Nodal and FGF pathways cooperate to maintain pluripotency of human embryonic stem cells. *J. Cell Sci.* **118**, 4495–4509 (2005).
62. Petrov, P. B., Considine, J. M., Izzi, V. & Naba, A. Matrisome AnalyzeR – a suite of tools to annotate and quantify ECM molecules in big datasets across organisms. *J. Cell Sci.* **136**, jcs261255 (2023).
63. Merkle, F. T. *et al.* Human pluripotent stem cells recurrently acquire and expand dominant negative P53 mutations. *Nature* **545**, 229–233 (2017).
64. Lezmi, E., Jung, J. & Benvenisty, N. High prevalence of acquired cancer-related mutations in 146 human pluripotent stem cell lines and their differentiated derivatives. *Nat. Biotechnol.* 1–5 (2024) doi:10.1038/s41587-023-02090-2.
65. Li, M. M. *et al.* Standards and Guidelines for the Interpretation and Reporting of Sequence Variants in Cancer: A Joint Consensus Recommendation of the Association for Molecular Pathology, American Society of Clinical Oncology, and College of American Pathologists. *J. Mol. Diagn. JMD* **19**, 4 (2017).
66. Bar, S., Schachter, M., Eldar-Geva, T. & Benvenisty, N. Large-Scale Analysis of Loss of Imprinting in Human Pluripotent Stem Cells. *Cell Rep.* **19**, 957–968 (2017).
67. Nazor, K. L. *et al.* Recurrent Variations in DNA Methylation in Human Pluripotent Stem Cells and their Differentiated Derivatives. *Cell Stem Cell* **10**, 620 (2012).
68. Rostovskaya, M., Stirparo, G. G. & Smith, A. Capacitation of human naïve pluripotent stem cells for multi-lineage differentiation. *Dev. Camb. Engl.* **146**, dev172916 (2019).
69. Zhao, C. *et al.* A Comprehensive Human Embryogenesis Reference Tool using Single-Cell RNA-Sequencing Data. 2021.05.07.442980 Preprint at https://doi.org/10.1101/2021.05.07.442980 (2024).
70. Cinkornpumin, J. K. *et al.* Naive Human Embryonic Stem Cells Can Give Rise to Cells with a Trophoblast-like Transcriptome and Methylome. *Stem Cell Rep.* **15**, 198–213 (2020).
71. Rostovskaya, M., Andrews, S., Reik, W. & Rugg-Gunn, P. J. Amniogenesis occurs in two independent waves in primates. *Cell Stem Cell* **29**, 744-759.e6 (2022).
72. Zorzan, I. *et al.* Chemical conversion of human conventional PSCs to TSCs following transient naive gene activation. *EMBO Rep.* **24**, e55235 (2023).
73. Yang, Y. *et al.* Heightened potency of human pluripotent stem cell lines created by transient BMP4 exposure. *Proc. Natl. Acad. Sci.* **112**, E2337–E2346 (2015).
74. Heidari Khoei, H. *et al.* Generating human blastoids modeling blastocyst-stage embryos and implantation. *Nat. Protoc.* **18**, 1584–1620 (2023).
75. Petropoulos, S. *et al.* Single-Cell RNA-Seq Reveals Lineage and X Chromosome Dynamics in Human Preimplantation Embryos. *Cell* **165**, 1012–1026 (2016).

1039 76. Xiang, L. *et al.* A developmental landscape of 3D-cultured human pre-gastrulation embryos.
1040 *Nature* **577**, 537–542 (2020).
1041 77. Meistermann, D. *et al.* Integrated pseudotime analysis of human pre-implantation embryo
1042 single-cell transcriptomes reveals the dynamics of lineage specification. *Cell Stem Cell* **28**,
1043 1625-1640.e6 (2021).
1044 78. Tyser, R. C. V. *et al.* Single-cell transcriptomic characterization of a gastrulating human
1045 embryo. *Nature* **600**, 285–289 (2021).
1046 79. Behringer, R., Gertsenstein, M., Nagy, K. V. & Nagy, A. Testing Serum Batches for Mouse
1047 Embryonic Stem Cell Culture. *Cold Spring Harb. Protoc.* **2017**, pdb.prot092411 (2017).
1048 80. Lazzarano, S. *et al.* Genetic mapping of species differences via in vitro crosses in mouse
1049 embryonic stem cells. *Proc. Natl. Acad. Sci.* **115**, 3680–3685 (2018).
1050 81. Yamanishi, A. *et al.* Collection of homozygous mutant mouse embryonic stem cells arising from
1051 autodiploidization during haploid gene trap mutagenesis. *Nucleic Acids Res.* **46**, e63 (2018).
1052 82. Acosta, S., Fiore, L., Carota, I. A. & Oliver, G. Use of two gRNAs for CRISPR/Cas9 improves
1053 bi-allelic homologous recombination efficiency in mouse embryonic stem cells. *genesis* **56**,
1054 e23212 (2018).
1055 83. Tamura, Y. *et al.* Homologous recombination is reduced in female embryonic stem cells by two
1056 active X chromosomes. *EMBO Rep.* **22**, e52190 (2021).
1057 84. Tsai, L.-K. *et al.* ZSCAN4 interacts with PARP1 to promote DNA repair in mouse embryonic
1058 stem cells. *Cell Biosci.* **13**, 193 (2023).
1059 85. Aflatoonian, B. *et al.* Generation of Sheffield (Shef) human embryonic stem cell lines using a
1060 microdrop culture system. *Vitro Cell. Dev. Biol. - Anim.* **46**, 236–241 (2010).
1061 86. Pantazis, C. B. *et al.* A reference human induced pluripotent stem cell line for large-scale
1062 collaborative studies. *Cell Stem Cell* **29**, 1685-1702.e22 (2022).
1063 87. Okae, H. *et al.* Derivation of Human Trophoblast Stem Cells. *Cell Stem Cell* **22**, 50-63.e6
1064 (2018).
1065 88. Io, S., Iemura, Y. & Takashima, Y. Optimized protocol for naive human pluripotent stem cell-
1066 derived trophoblast induction. *STAR Protoc.* **2**, 100921 (2021).
1067 89. Rivron, N. C. *et al.* Tissue deformation spatially modulates VEGF signaling and angiogenesis.
1068 *Proc. Natl. Acad. Sci. U. S. A.* **109**, 6886–6891 (2012).
1069 90. Pasque, V. *et al.* X Chromosome Reactivation Dynamics Reveal Stages of Reprogramming to
1070 Pluripotency. *Cell* **159**, 1681–1697 (2014).
1071 91. Michalski, A. *et al.* Mass Spectrometry-based Proteomics Using Q Exactive, a High-
1072 performance Benchtop Quadrupole Orbitrap Mass Spectrometer*. *Mol. Cell. Proteomics* **10**,
1073 M111.011015 (2011).
1074 92. Freed, D., Aldana, R., Weber, J. A. & Edwards, J. S. The Sentieon Genomics Tools - A fast and
1075 accurate solution to variant calling from next-generation sequence data. 115717 Preprint at
1076 https://doi.org/10.1101/115717 (2017).
1077 93. McLaren, W. *et al.* The Ensembl Variant Effect Predictor. *Genome Biol.* **17**, 122 (2016).
1078 94. Patro, R., Duggal, G., Love, M. I., Irizarry, R. A. & Kingsford, C. Salmon provides fast and
1079 bias-aware quantification of transcript expression. *Nat. Methods* **14**, 417–419 (2017).
1080 95. Soneson, C., Love, M. I. & Robinson, M. D. Differential analyses for RNA-seq: transcript-level
1081 estimates improve gene-level inferences. Preprint at
1082 https://doi.org/10.12688/f1000research.7563.2 (2016).
1083 96. Robinson, M. D., McCarthy, D. J. & Smyth, G. K. edgeR: a Bioconductor package for
1084 differential expression analysis of digital gene expression data. *Bioinformatics* **26**, 139–140
1085 (2010).
1086 97. Hansen, S. L. *et al.* An organoid-based CRISPR-Cas9 screen for regulators of intestinal
1087 epithelial maturation and cell fate. *Sci. Adv.* **9**, eadg4055 (2023).
1088 98. Hao, Y. *et al.* Integrated analysis of multimodal single-cell data. *Cell* **184**, 3573-3587.e29
1089 (2021).
1090 99. Tirosh, I. *et al.* Dissecting the multicellular ecosystem of metastatic melanoma by single-cell
1091 RNA-seq. *Science* **352**, 189–196 (2016).
1092 100. Marthandan, S. *et al.* Similarities in Gene Expression Profiles during In Vitro Aging of Primary
1093 Human Embryonic Lung and Foreskin Fibroblasts. *BioMed Res. Int.* **2015**, 731938 (2015).

1094 101. Chen, D. *et al.* Transcriptomic profiles of human foreskin fibroblast cells in response to orf
1095 virus. *Oncotarget* **8**, 58668–58685 (2017).
1096 102. Jang, Y. J., Kim, M., Lee, B.-K. & Kim, J. Induction of human trophoblast stem-like cells from
1097 primed pluripotent stem cells. *Proc. Natl. Acad. Sci.* **119**, e2115709119 (2022).
1098 103. Wei, Y. *et al.* Efficient derivation of human trophoblast stem cells from primed pluripotent stem
1099 cells. *Sci. Adv.* **7**, eabf4416 (2021).
1100 104. Zorzan, I. *et al.* The transcriptional regulator ZNF398 mediates pluripotency and epithelial
1101 character downstream of TGF-beta in human PSCs. *Nat. Commun.* **11**, 2364 (2020).
1102 105. Choi, J. *et al.* A comparison of genetically matched cell lines reveals the equivalence of human
1103 iPSCs and ESCs. *Nat. Biotechnol.* **33**, 1173–1181 (2015).
1104 106. Guo, G. *et al.* Epigenetic resetting of human pluripotency. *Development* **144**, 2748–2763 (2017).
1105 107. MacCarthy, C. M. *et al.* Highly cooperative chimeric super-SOX induces naive pluripotency
1106 across species. *Cell Stem Cell* **31**, 127-147.e9 (2024).

1107 **Figure Legends**

1108 **FIGURE 1**

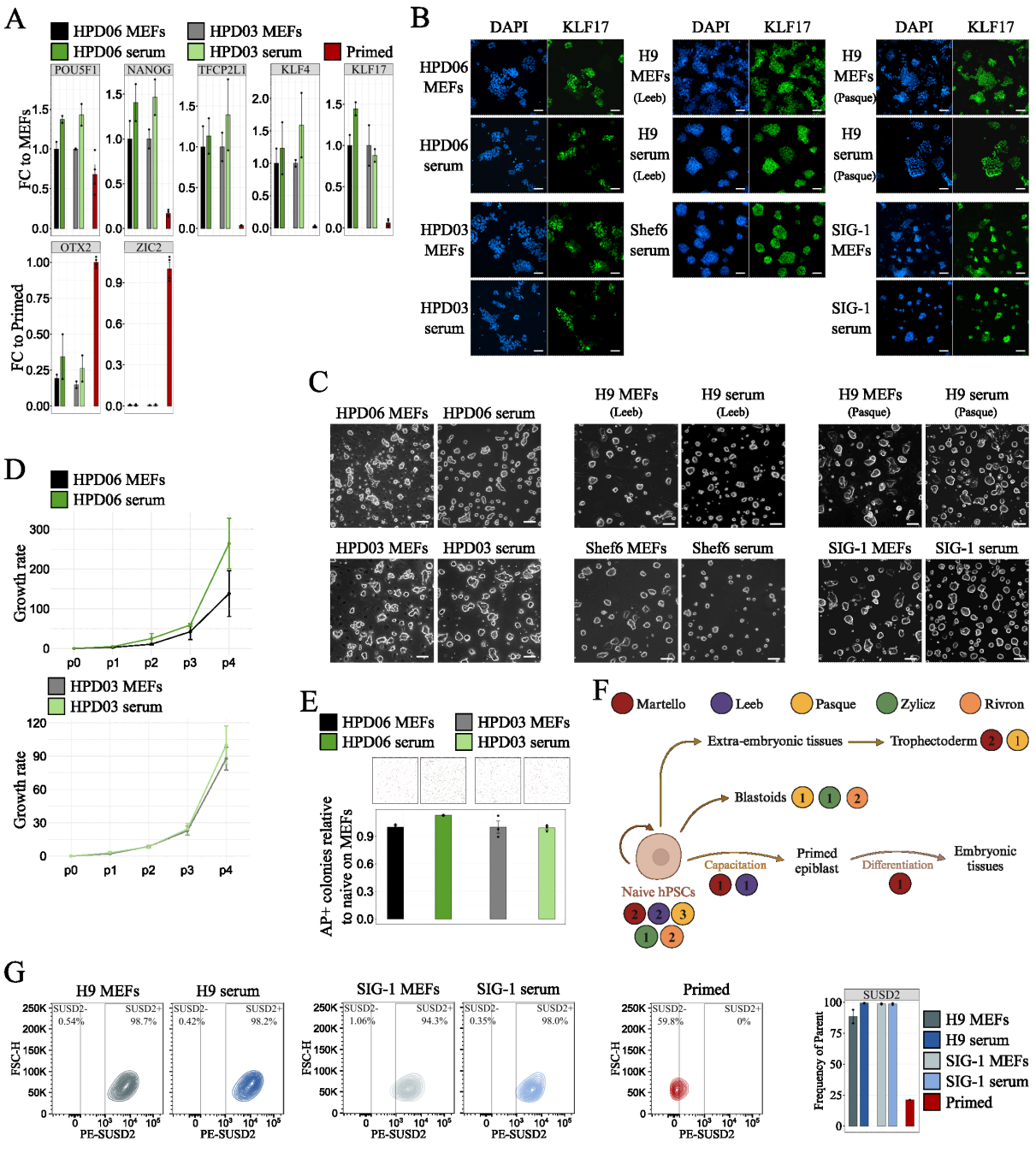

1109

1110 **FIGURE 1 - Serum coating allows for the maintenance of naive hPSCs**

1111 **A** Gene expression analysis by RT-qPCR of general (*POU5F1* and *NANOG*), naive (*TFCP2L1*, *KLF4*
1112 and *KLF17*) and primed (*OTX2* and *ZIC2*) pluripotency markers in HPD06 and HPD03 naive hiPSCs
1113 stably cultured on MEFs, serum or matrigel coating. Bars indicate the mean ± SEM of biological
1114 replicates shown as dots. n = 2 from independent experiments for naive hiPSCs and n = 4 from
1115 independent experiments for primed hPSCs.

1116 **B** Immunostaining for KLF17 of different naive hPSC lines (HPD06, HPD03 and SIG-1 iPSCs, and H9
1117 and Shef6 ESCs) stably cultured on MEFs or serum coating. See also Supplementary Figure 1B-C.
1118 Scale bars: 100 µM. Representative images of two independent experiments are shown.

1119 **C** Morphologies of different naive hPSC lines (HPD06, HPD03 and SIG-1 iPSCs, and H9 and Shef6
1120 ESCs) stably cultured on MEFs or serum coating. Scale bars: 100 µm. Representative images of two
1121 independent experiments are shown.

1122 **D** Growth rate of HPD06 and HPD03 naive hiPSCs stably cultured on MEFs or serum coating. Bars
1123 indicate the mean ± SEM of n = 2 independent experiments shown as dots.

1124 **E** Top: Representative AP staining images after clonal assay of HPD06 and HPD03 naive hiPSCs stably
1125 cultured on MEFs or serum coating. Bottom: Quantification of the relative number of AP-positive
1126 pluripotent colonies counted per well. Bars indicate the mean ± SEM of n = 3 independent experiments
1127 shown as dots.

1128 **F** Schematic representation of the analyses performed in this study. Coloured dots identify the
1129 laboratories involved, with numbers indicating cell lines used for each analysis.

1130 **G** Flow cytometry analysis of naive H9 hESCs and SIG-1 hiPSCs stably cultured on MEFs or serum
1131 coating. Left: Representative contour plots of SUSD-PE *versus* forward scatter. Right: Quantification
1132 of SUSD2 positive cells as the frequency of live cells. Bars indicate the mean ± SEM of n = 2 technical
1133 replicates shown as dots.

FIGURE 2

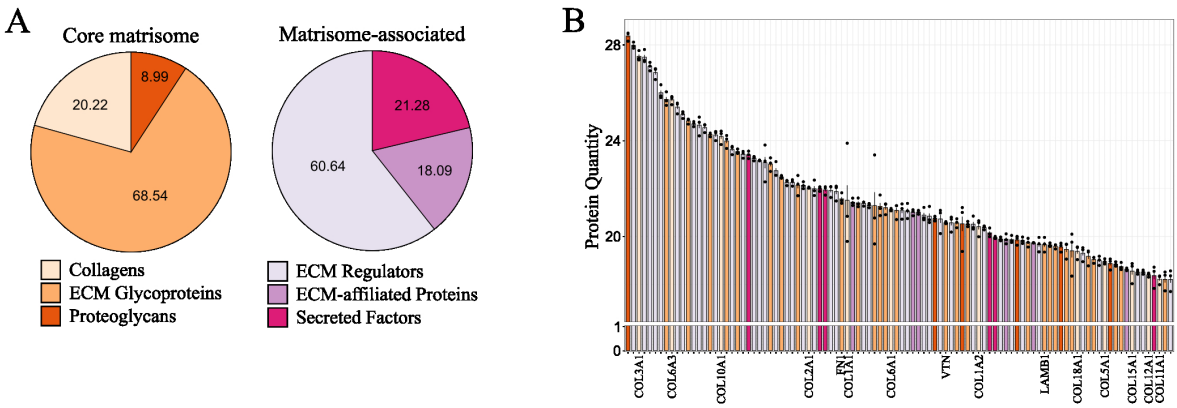

FIGURE 2 - Serum contains a mixture of ECM proteins

A ECM proteins enrichment analysis of the serum coating proteome. Left: Composition of core matrisome proteins expressed in percentage. Right: Composition of matrisome-associated proteins expressed in percentage.

B Top 100 most abundant proteins of the serum coating. Commonly used surface coatings for feeder-free cultures and detected collagens are highlighted. Bars indicate the mean ± SEM of n = 3 technical replicates shown as dots.

1143 **FIGURE 3**

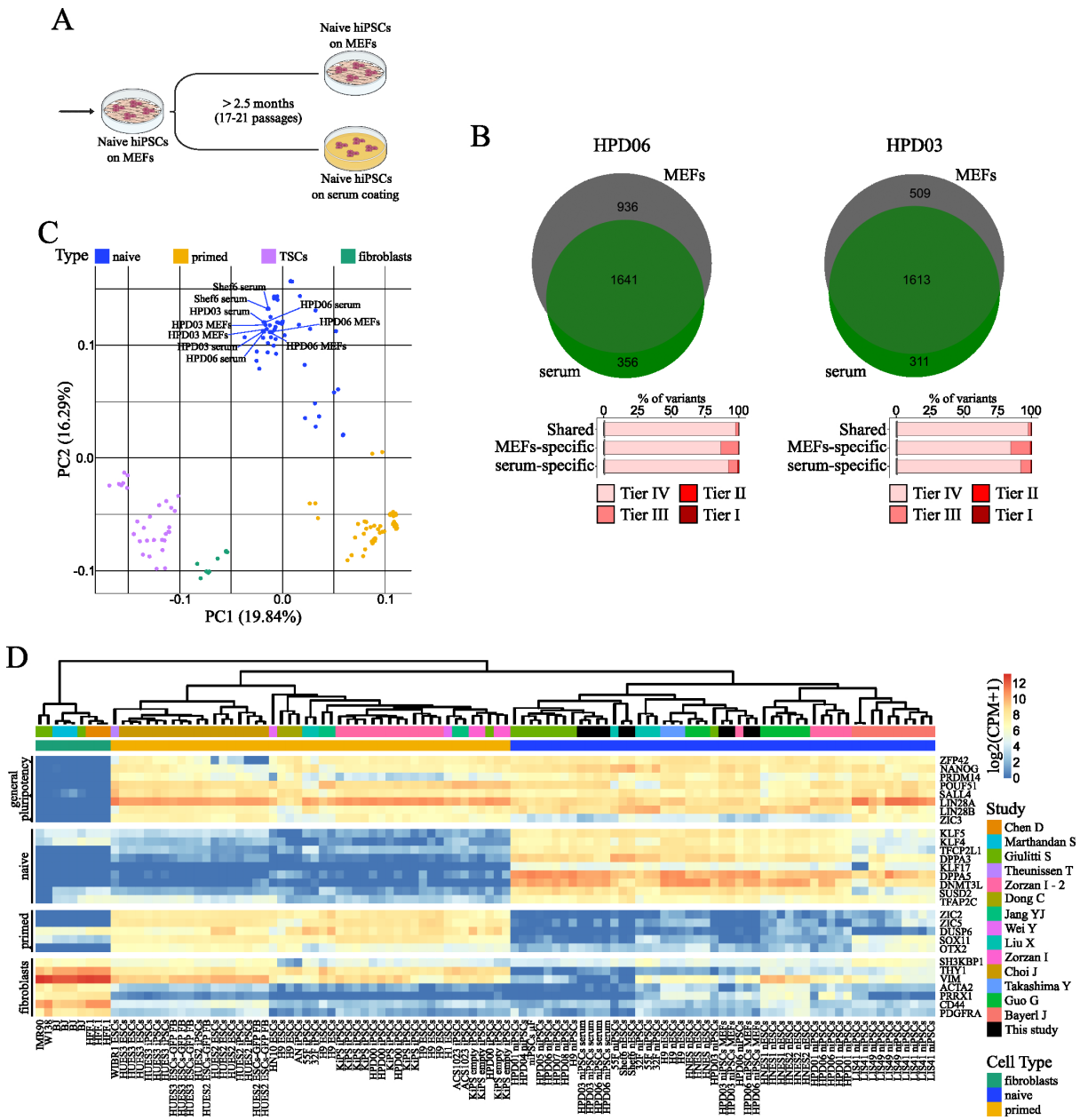

1144

1145 **FIGURE 3 - Naive hPSCs on serum coating do not accumulate pathogenic**
1146 **mutations and maintain their transcriptomic profile**

1147 **A** Schematic representation of the experimental setting for the Exome-Seq analysis of HPD06 and
1148 HPD03 naive hiPSCs stably cultured on MEFs or serum coating.
1149 **B** Analysis of detected genetic variations in coding genes of HPD06 and HPD03 naive hiPSCs stably
1150 cultured on MEFs or serum coating compared to the reference human genome. Top: Venn diagrams
1151 showing the quantification of shared and culture-specific (MEFs or serum coating) detected variants
1152 and mutated genes identified in each condition. All Tier II detected genes and genes identified as
1153 commonly mutated in hPSCs[64] are highlighted. Bottom: Barplots of the composition of shared and
1154 culture-specific (MEFs or serum coating) detected variants classified by Tier and expressed in
1155 percentage.
1156 **C** Principal component analysis of naive hPSC lines (HPD06 and HPD03 hiPSCs, and Shef6 hESCs)
1157 stably cultured on MEFs or serum coating with published naive and primed hPSCs, TSCs and fibroblast
1158 lines performed on the top 5,000 most variable genes identified through RNA-seq.
1159 **D** Heatmap of general pluripotency, naive, primed, and fibroblasts genes in naive hPSC lines (HPD06
1160 and HPD03 hiPSCs, and Shef6 hESCs) stably cultured on MEFs or serum coating and in published
1161 fibroblasts, primed hPSCs and naive hPSCs.

FIGURE 4

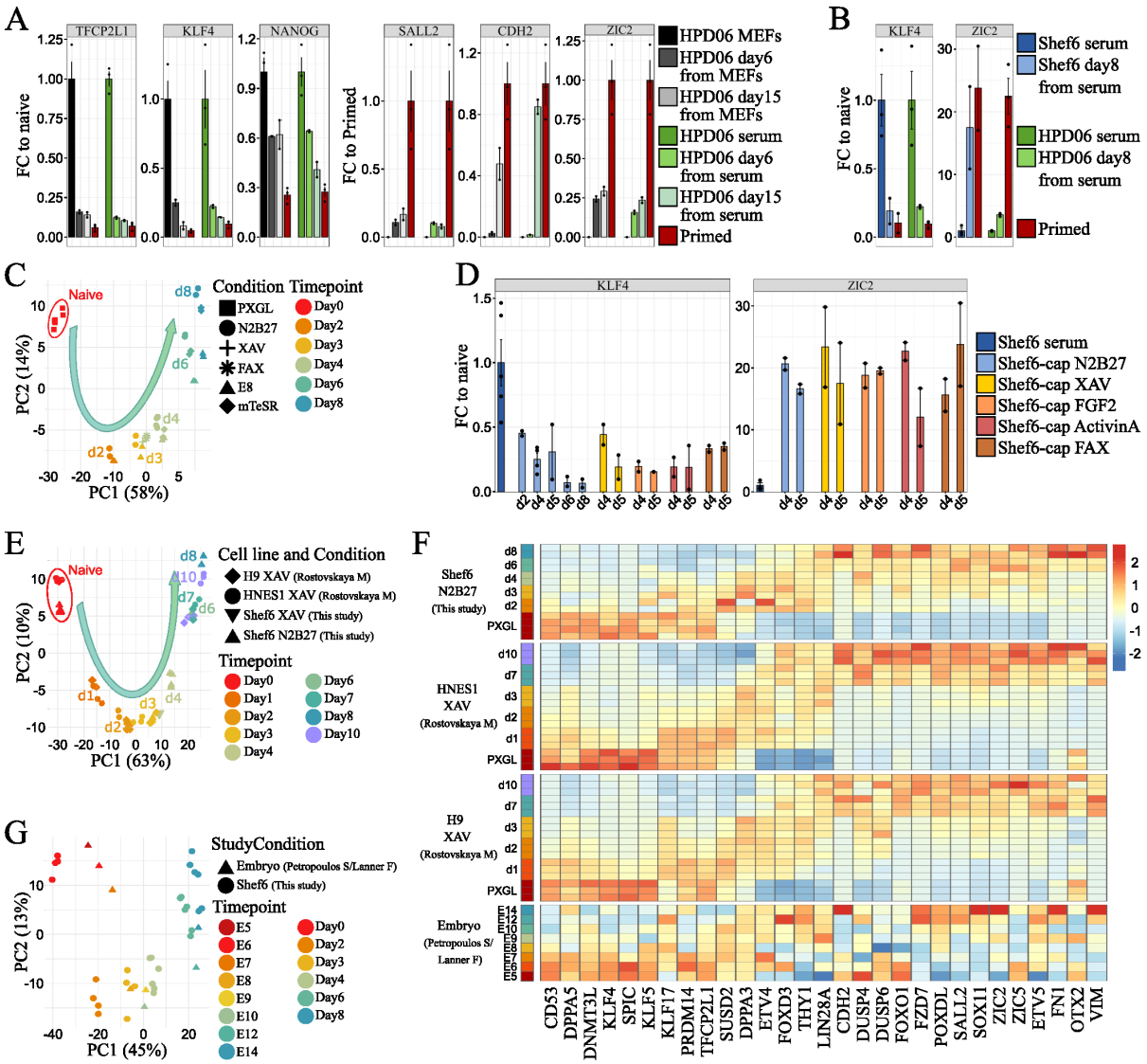
A
TFCP2L1
KLF4
NANOG
SALL2
CDH2
ZIC2
FC to naive
FC to Primed
HPD06 MEFs
HPD06 day6 from MEFs
HPD06 day15 from MEFs
HPD06 serum
HPD06 day6 from serum
HPD06 day15 from serum
Primed
B
KLF4
ZIC2
FC to naive
Shef6 serum
Shef6 day8 from serum
HPD06 serum
HPD06 day8 from serum
Primed
C
Naive
d8
d6
d4
d2
d3
PC2 (14%)
PC1 (58%)
Condition Timepoint
PXGL
N2B27
XAV
FAX
E8
mTeSR
Day0
Day2
Day3
Day4
Day6
Day8
D
KLF4
ZIC2
FC to naive
Shef6 serum
Shef6-cap N2B27
Shef6-cap XAV
Shef6-cap FGF2
Shef6-cap ActivinA
Shef6-cap FAX
E
Naive
d8
d10
d7
d6
d1
d3
d4
d2
PC2 (10%)
PC1 (63%)
Cell line and Condition
H9 XAV (Rostovskaya M)
HNES1 XAV (Rostovskaya M)
Shef6 XAV (This study)
Shef6 N2B27 (This study)
Timepoint
Day0
Day1
Day2
Day3
Day4
Day6
Day7
Day8
Day10
F
Shef6 N2B27 (This study)
HNES1 XAV (Rostovskaya M)
H9 XAV (Rostovskaya M)
Embryo (Petropoulos S/ Lanner F)
PXGL
CD53
DPPA5
DNMT3L
KLF4
SPIC
KLF5
KLF17
PRDM14
TFCP2L1
SUSD2
DPPA3
ETV4
FOXD3
THY1
LIN28A
CDH2
DUSP4
DUSP6
FOXO1
FZD7
POXDL
SALL2
SOX11
ZIC2
ZIC5
ETV5
FN1
OTX2
VIM
G
PC2 (13%)
PC1 (45%)
StudyCondition
Embryo (Petropoulos S/Lanner F)
Shef6 (This study)
Timepoint
E5
E6
E7
E8
E9
E10
E12
E14
Day0
Day2
Day3
Day4
Day6
Day8

1164 **FIGURE 4 - Feeder-free naive hPSCs can recapitulate embryonic**
1165 **differentiation trajectories**

1166 **A** Gene expression analysis by RT-qPCR of naive (*TFCP2L1* and *KLF4*), general (*NANOG*) and primed
1167 (*SALL2*, *CDH2* and *ZIC2*) pluripotency markers in HDP06 hiPSCs capacitated from naive lines stably
1168 cultured on MEFs or serum coating. Bars indicate the mean ± SEM of biological replicates shown as
1169 dots. Biological replicates include n = 3 from three independent experiments for naive hPSCs in PXGL
1170 and primed and n = 2 from two independent experiments for capacitated cells at days 6 and 15.
1171 **B** Gene expression analysis by RT-qPCR of naive (*KLF4*) and primed (*ZIC2*) pluripotency markers in
1172 Shef6 hESCs and HDP06 hiPSCs capacitated from naive lines stably cultured on serum coating. Bars
1173 indicate the mean ± SEM of biological replicates shown as dots. Biological replicates include n = 3 from
1174 three independent experiments for naive hPSCs, n = 2 from two independent experiments for
1175 capacitated cells at day 8, and n = 2 or 3 from two or three independent experiments for primed hPSCs.
1176 **C** Principal component analysis of all genes identified via RNA-seq of an eight-day differentiation time
1177 course starting from Shef6 naive hESCs stably cultured on serum coating in PXGL. Differentiation was
1178 induced by culture in basal medium (N2B27) with or without supplementation of TNKS1/2 inhibition
1179 (XAV) or FGF2-ActivinA-XAV (FAX) or commercial media containing FGF2 and Activin A
1180 signalling modulators (E8 or mTeSR). Biological replicates include n = 6 from two independent
1181 experiments for d0, from two independent experiments n = 4 for N2B27 at day 4, and n = 2 for all other
1182 combinations of conditions and time points.
1183 **D** Gene expression analysis by RT-qPCR of naive (*KLF4*) and primed (*ZIC2*) pluripotency markers of
1184 Shef6 naive hESCs stably cultured on serum coating and capacitated in basal medium (N2B27)
1185 supplemented with XAV, FGF2, Activin A or a combination of all three (FAX). Bars indicate the
1186 mean ± SEM of relative expression levels ($2^{-\Delta\Delta CT}$) calculated for biological replicates shown as dots.
1187 Biological replicates include n = 5 from two independent experiments for naive cells on serum, n = 4
1188 from two independent experiments for N2B27 at day 4, and n = 2 for all other combinations of
1189 conditions and time points.
1190 **E** Principal component analysis of the abovementioned feeder-free eight-day differentiation time course
1191 in N2B27 with or without supplementation of XAV integrated with already published RNA-seq data of
1192 H9 and HNES1 hESCs cultured on MEFs and capacitated in N2B27 supplemented with XAV for up to
1193 10 days[68]. Data was batch-corrected for data sets. Biological replicates include n = 6 from two
1194 independent experiments for d0, n = 4 from two independent experiments for N2B27 at day 4, n = 2 for
1195 all other combinations of conditions and time points, and n = 3 for each combination of cell line,
1196 condition, and timepoint in the published dataset.
1197 **F** Heatmaps showing the expression of general pluripotency, naive, and primed markers. *In vitro* data
1198 includes serum-adapted Shef6 naive hESC lines capacitated in N2B27 and published data for H9 and
1199 HNES1 hESCs cultured on MEFs and capacitated in N2B27 supplemented with XAV[68]. Biological

replicates include n = 6 from two independent experiments for PXGL, n = 4 from two independent experiments for N2B27 at day 4, n = 2 for all other combinations of conditions and time points, and n = 3 for each combination of cell line, condition, and timepoint in the published dataset. The human embryo reference dataset was a subset for embryonic cells spanning E5-E14[75]. Expression levels for bulk data are row-wise z-transformed DESeq2-normalized counts. For the embryo data expression values were normalised, averaged and then log-transformed.

G Principal component analysis of the abovementioned feeder-free eight-day differentiation time course (N2B27, E8 and mTeSR) integrated with pseudo bulk data derived from the human embryo reference dataset (subset for embryonic cells spanning E5-E14). Data was batch-corrected for data sets and then filtered by the 9376 DEGs (|log2FC| > 1, padj < 0.05) when comparing the naive state with any of the differentiation conditions and time points. Biological replicates include n = 4 from two independent experiments for d0 and n = 2 for all other combinations of conditions and time points.

1212 **FIGURE 5**

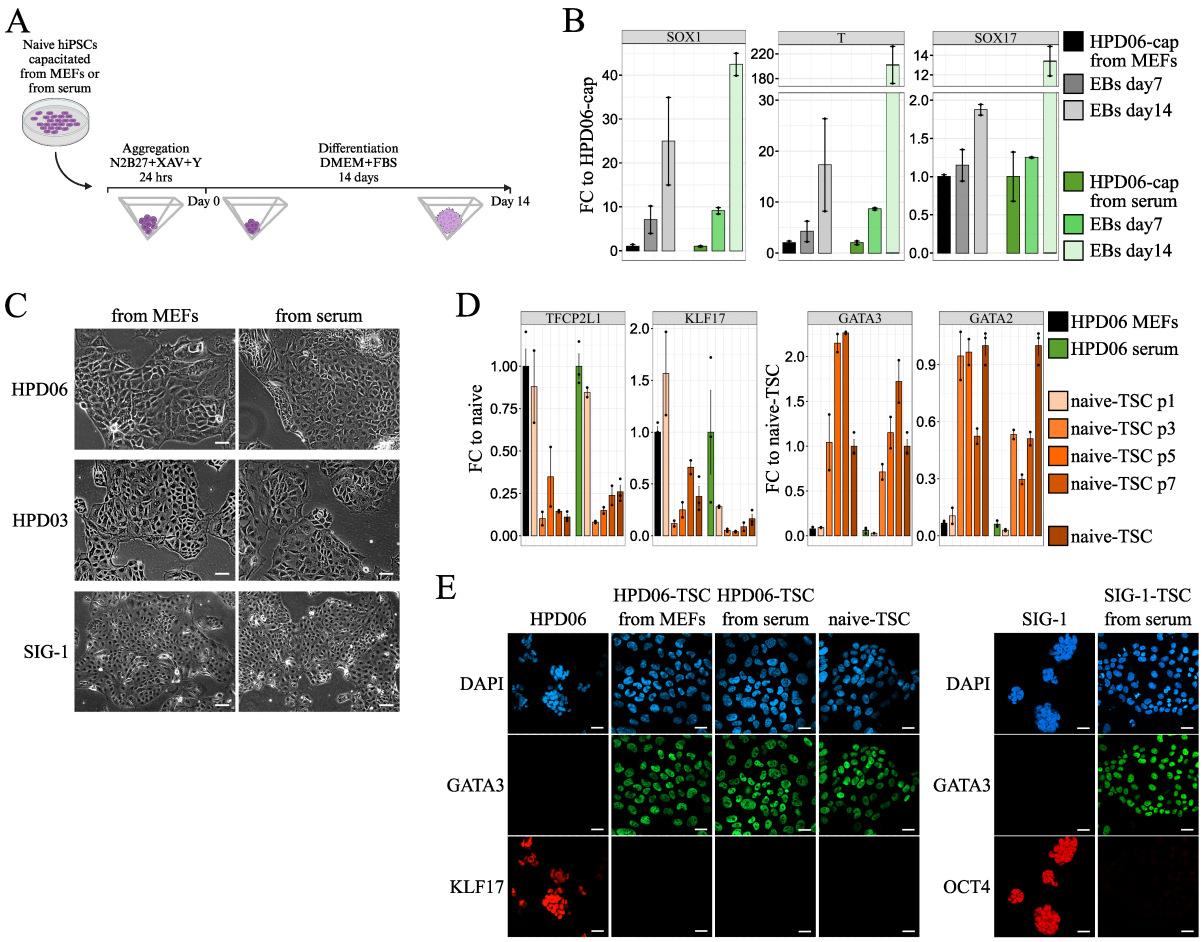

1213

1214 **FIGURE 5 - Feeder-free naive hPSCs efficiently differentiate to embryonic**
1215 **and extraembryonic lineages**

1216 **A** Schematic representation of the experimental setting for the EBs differentiation of HPD06 naive
1217 hiPSCs capacitated from MEFs or serum coating.
1218 **B** Gene expression analysis by RT-qPCR of germ layers markers (*SOX1*, *T*, and *SOX17*) in EBs derived
1219 from capacitated HPD06 naive hiPSCs capacitated from MEFs or serum coating. Bars indicate the
1220 mean ± SEM of n = 2 independent experiments biological replicates shown as dots.
1221 **C** Morphologies of TSCs derived from HPD06, HPD03 and SIG-1 naive hiPSCs stably cultured on
1222 MEFs or serum coating. Scale bars: 50 µm. Representative images of two biological replicates.
1223 **D** Gene expression analysis by RT-qPCR of naive pluripotency (*TFCP2L1* and *KLF17*) and TSCs
1224 (*GATA3* and *GATA2*) markers in TSCs derived from HPD06 naive hiPSCs stably cultured on MEFs or
1225 serum coating. Bars indicate the mean ± SEM of technical replicates shown as dots. Biological
1226 replicates include n = 3 independent experiments for naive hPSCs and naive-TSCs and n = 2
1227 independent experiments for the differentiation time points.
1228 **E** Immunostaining for TSCs (GATA3) and naive (KLF17) or general pluripotency (OCT4) markers of
1229 trophectoderm derived from HPD06 and SIG-1 naive hiPSCs stably cultured on MEFs or serum coating.
1230 Scale bars: 50 µM. Representative images of two independent experiments are shown.

FIGURE 6

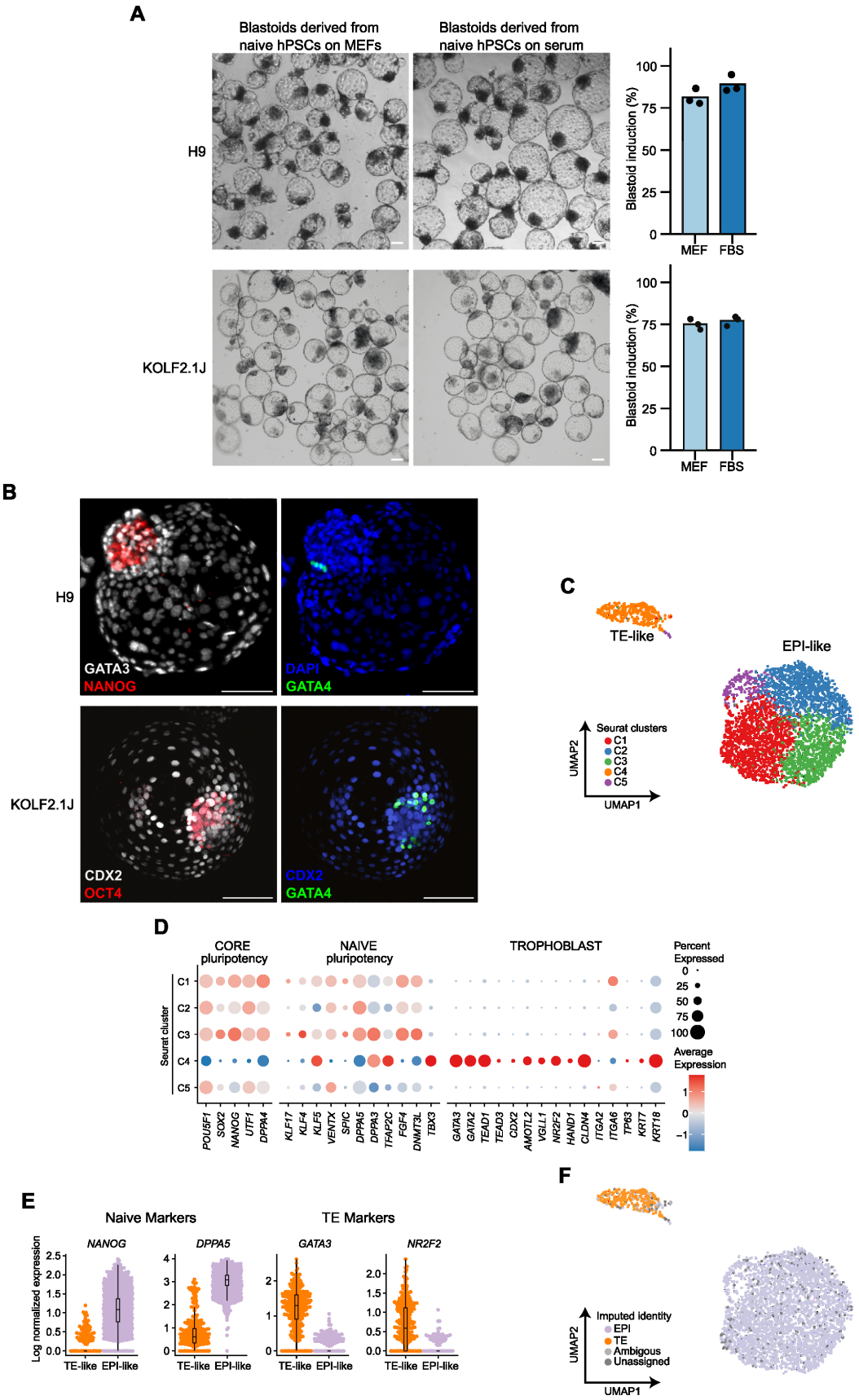
A
Blastoids derived from naive hPSCs on MEFs
Blastoids derived from naive hPSCs on serum
H9
KOLF2.1J
Blastoid induction (%)
100
75
50
25
0
MEF
FBS
B
H9
KOLF2.1J
GATA3
NANOG
DAPI
GATA4
CDX2
OCT4
CDX2
GATA4
C
TE-like
EPI-like
Seurat clusters
C1
C2
C3
C4
C5
UMAP2
UMAP1
D
CORE pluripotency
NAIVE pluripotency
TROPHOBLAST
Percent Expressed
Average Expression
Seurat cluster
POU5F1
SOX2
NANOG
UTF1
DPPA4
KLF17
KLF4
KLF5
VENTX
SPIC
DPPA5
DPPA3
TFAP2C
FGF4
DNMT3L
TBX3
GATA3
GATA2
TEAD1
TEAD3
CDX2
AMOTL2
VGLL1
NR2F2
HAND1
CLDN4
ITGA2
ITGA6
TP63
KRT7
KRT18
E
Naive Markers
TE Markers
NANOG
DPPA5
GATA3
NR2F2
Log normalized expression
TE-like
EPI-like
F
Imputed Identity
EPI
TE
Ambigous
Unassigned
UMAP2
UMAP1

1233 **FIGURE 6 - Feeder-free naive hPSCs efficiently form blastoids**

1234 **A** Left: Representative brightfield images of blastoids induced from naive H9 hESC and naive
1235 KOLF2.1J hiPSCs cultured on MEFs or serum coating. Scale bar: 100 µm. Right: quantification of
1236 induction efficiency from naive H9 hESC and naive KOLF2.1J hiPSCs cultured on MEFs or serum-
1237 coated dishes. Data is based on brightfield images of d5 blastoids. Data is presented as the mean and
1238 data points of n = 3 biological replicates for naive H9 hESC and n = 3 technical replicates for naive
1239 KOLF2.1J hiPSCs.

1240 **B** Immunostaining of d5 blastoids derived from naive H9 hESC and naive KOLF2.1J hiPSCs cultured
1241 on serum coating. Blastoids were stained for TE (GATA3 or CDX2), PrE (GATA4) and EPI (NANOG
1242 and OCT4) markers. Shown is the maximum projection. Scale bars: 100 µm.

1243 **C** UMAP plot from scRNA-seq analysis of blastoids from naive H9 hESCs cultured on serum coating.
1244 Cells are coloured according to the sample Seurat cluster (n = 3260). Highlighted are TE-like (cluster
1245 4) and EPI-like clusters.

1246 **D** Expression of selected lineage-specific marker genes across Seurat clusters from (C). The size of the
1247 dots represents the proportion of cells in the indicated group expressing the given gene and colour
1248 encodes the scaled average expression.

1249 **E** Combined beeswarm and box plots of gene expression of naive pluripotency markers (*NANOG* and
1250 *DPPA5*) and TE markers (*GATA3* and *NR2F2*) from (C). Cells were separated based on their EPI or TE
1251 signature. Single cells are plotted as dots; boxes span the interquartile range (IQR), the centre line
1252 indicates the median and whiskers extend to values within 1.5 times the IQR.

1253 **F** UMAP plots as in (C) but with cells based on the imputed annotation of *in vitro* samples from a
1254 reference in vivo dataset[69]. Unassigned and ambiguous labels refer to cells with either none or with
1255 more than two imputed annotations respectively.

1256 **TABLE 1 - Naive hPSC lines used in this study:**

Cell line	Origin	Sex	Derivation	Group
HPD06	Induced from human fibroblasts	Male	Somatic cell reprogramming[30]	Martello
HPD03	Induced from human fibroblasts	Male	Somatic cell reprogramming[30]	Martello
H9[1]	Embryonic	Female	Epigenetic resetting[106]	Leeb
Shef6[85]	Embryonic	Female	Epigenetic resetting[106]	Leeb
H9[1]	Embryonic	Female	Epigenetic resetting[106]	Pasque
SIG-1	Induced from human fibroblasts	Female	mRNA KLF4 reprogramming[27]	Pasque
HNES1	Embryonic	Male	From blastocyst[26]	Pasque
H9[1]	Embryonic	Female	Epigenetic resetting[106]	Zylicz
KOLF2.1J	Induced from human fibroblasts	Male	Episomal Sox2-17 and KLF4 reprogramming[107]	Rivron
SCTi003-A	Induced from human fibroblasts	Female	Episomal Sox2-17 and KLF4 reprogramming[107]	Rivron

1257

1258 **Supplementary Material**

1259 **Supplementary Table 1 - Primers used in this study:**

Group	Target	Sequence
Martello Group	POU5F1_FW POU5F1_RW	GTGGAGGAAGCTGACAACAA ATTCTCCAGGTTGCCTCTCA
	NANOG_FW NANOG_RV	CAAAGGCAAACAACCCACTT TCTGCTGGAGGCTGAGGTAT
	TFCP2L1_FW TFCP2L1_RW	GGAGTTCCAGCCATGCTCTT CCTGCTTGAAGATGGGCAGA
	KLF4 _FW KLF4 _RV	CCCAATTACCCATCCTTCCT CAGGTGTGCCTTGAGATGG
	KLF17_FW KLF17_RV	CACACAGGTGAGAGGCCATA ACTCGGTGTGTACCCGCATA
	OTX2_FW OTX2_RV	GAGAGGAGGTGGCACTGAAA TGACCTCCATTCTGCTGTTG
	ZIC2_FW ZIC2_RV	CATGCACGTCCACACCTC CTCATGGACCTTCATGTGCTT
	SALL2_FW SALL2_RV	GCACGAATCCGAGAGGAG TCACCATTACAGGAGGGTCAG
	CDH2_FW CDH2_RV	CGTGGTCAAACCAATCGAC AACAGACACGGTTGCAGTTG
	GATA3_FW GATA3_RV	ACAGAAGGCAGGGAGTGTGT TCCGTTCATTTTGTGATAGAGC
	GATA2_FW GATA2_RV	GACTACAGCAGCGGACTCTT GCCTTCTGAACAGGAACGAG
	IGFBP3_FW IGFBP3_RV	CCTGCCGTAGAGAAATGGAA AAGGGCGACACTGCTTTTT
	BAMBI_FW BAMBI_RV	GAGGCCTCAGGACAAGGAAA CCCGGAACCACAACTCTTT
	SOX1_FW SOX1_RV	GCTGACACCAGACTTGGGTTT CCCCTCGAGCAAAGAAAACG
	T_FW T_RV	GCCAGATCATGCTGAACTCC AAGCTTTTGCAAATGGATTGT
	SOX17_FW SOX17_RV	ACGCCGAGTTGAGCAAGA TCTGCCTCCTCCACGAAG
	GAPDH_FW GAPDH_RV	GCCTCAAGATCATCAGCAATGC CGCCACAGTTTCCCGGAG
Leeb group	KLF4_FW KLF4_RV	CCCACATGAAGCGACTTCCC CAGGTCCAGGAGATCGTTGAA
	ZIC2_FW ZIC2_RV	CATGCACGGTCCACACCTC CTCATGGACCTTCATGTGCTT
	ACTB_FW ACTB_RV	CCAACCGCCGAGAAGATGA CCAGCGGCGTACAGGGATAG

1260

1261 **Supplementary Table 2 - Primary antibodies used in this study:**

Group	Target	Conjugate	Supplier	Catalog ID	IF dil.
Martello Group	KLF17	-	Atlas Antibodies	HPA024629	1:250
	OCT4 (C-10)	-	Santa Cruz	sc-5279	1:300
	NANOG	-	Cell Signaling	D73G4	1:100
	TFCP2L1	-	R&D Systems	AF5726	1:250
	GATA3	-	R&D Systems	AF2605	1:100
Leeb Group	KLF17	-	Atlas Antibodies	HPA024629	1:333
	OCT4 (C-10)	-	Santa Cruz	sc5279	1:50
	SUSD2 (W5C5)	APC	BioLegend	327408	1:100
Pasque Group	KLF17	-	Abcam	HPA024629	1:300
	OCT4 (C-10)	-	Santa Cruz	sc-5279	1:100
	NANOG	-	BD Bioscience	560482	1:50
	GATA3		R&D System	AF2605	1:100
	SOX17	-	R&D System	AF1924	1:100
	SUSD2	PE	Biolegend	327406	1:50
	GATA2	-	Sigma-Aldrich	WH0002624M1	1:100
	NANOG	-	Abcam	ab21624	1:100
Zylicz Group	NANOG	-	Abcam	ab173368	1:250
	GATA3	-	Abcam	ab199428	1:250
	GATA4	-	eBioscience	14-9980-80	1:250
Rivron Lab	OCT4 (C-10)	-	Santa Cruz	sc-5279	1:200
	CDX2	-	Abcam	ab76541	1:1000
	GATA4	-	Invitrogen	14-9980-82	1:400

1262

SUPPLEMENTARY FIGURE 1

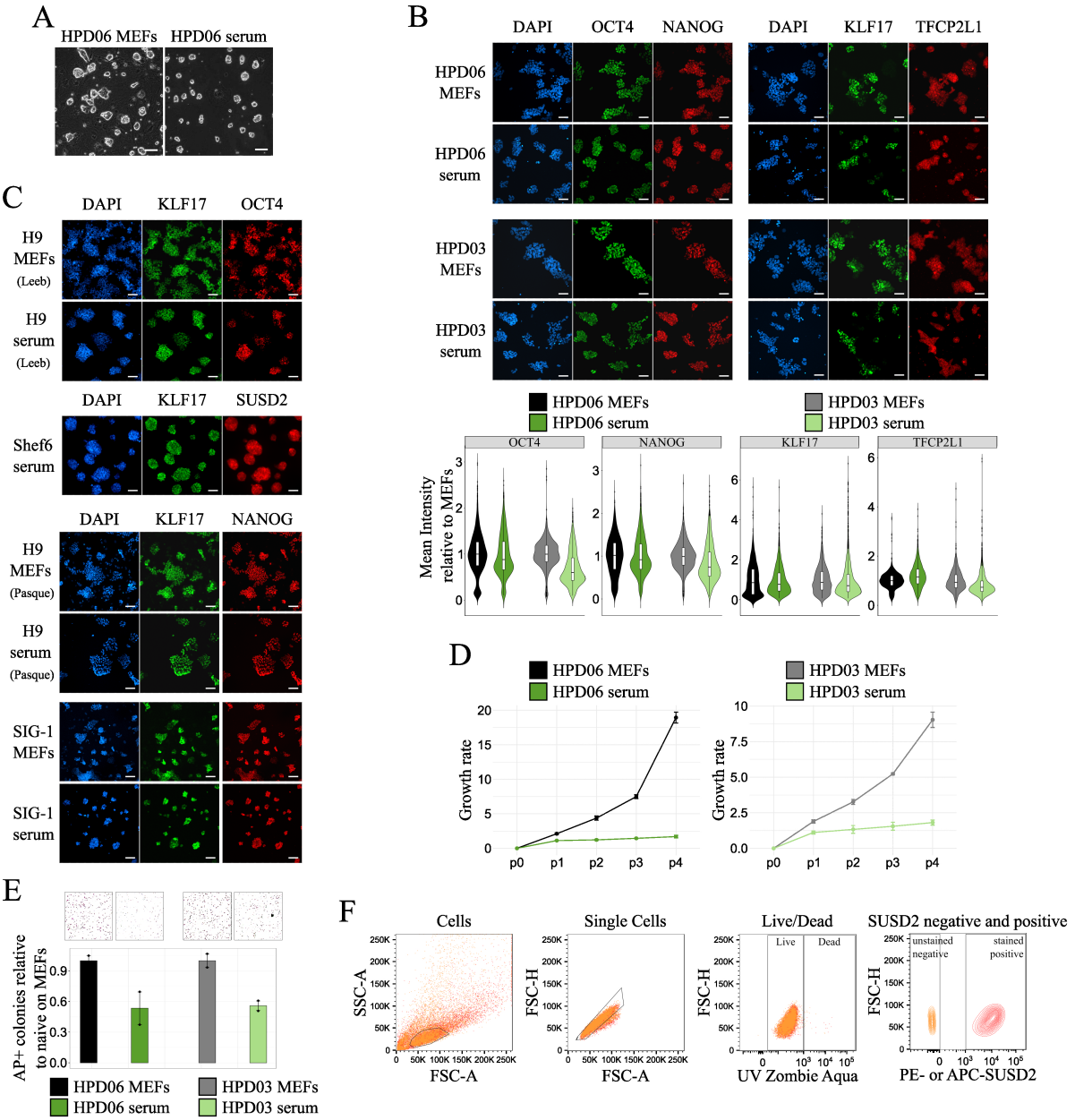

1265 # SUPPLEMENTARY FIGURE 1

1266 **A** Morphologies of HPD06 naive hiPSC line cultured on MEFs or serum coating at the 4th passage
1267 when plated at a low density. Scale bars: 100 µm. Representative images of two independent
1268 experiments are shown.
1269 **B** Top: Immunostaining for general pluripotency (OCT4 and NANOG) and naive (KLF17 and
1270 TFCP2L1) markers of HPD06 and HPD03 naive hiPSCs cultured on MEFs or serum coating at the 4th
1271 passage. Complete view of Figure 1B. Scale bars: 100 µM. Representative images of two independent
1272 experiments are shown. Bottom: Mean fluorescence intensity quantification for general pluripotency
1273 (OCT4 and NANOG) and naive (KLF17 and TFCP2L1) markers of HPD06 and HPD03 naive hiPSCs
1274 cultured on MEFs or serum coating at the 4th passage. At least 700 nuclei from five randomly selected
1275 fields from two independent experiments were analysed for each condition. The box plot indicates the
1276 25th, 50th and 75th percentiles.
1277 **C** Immunostaining for general pluripotency (OCT4 and NANOG) and naive (KLF17 and SUSD2)
1278 markers of H9 and Shef6 naive hESCs, and SIG-1 hiPSCs stably cultured on MEFs or serum coating.
1279 Complete view of Figure 1B. Scale bars: 100 µM. Representative images of two independent
1280 experiments are shown.
1281 **D** Growth rate of HPD06 and HPD03 naive hiPSCs cultured on MEFs or serum coating when plated at
1282 a low density over the first 4 passages of the conversion. Bars indicate the mean ± SEM of n = 2
1283 independent experiments shown as dots.
1284 **E** Top: Representative AP staining images after clonal assay of HPD06 and HPD03 naive hiPSCs
1285 cultured on MEFs or serum coating when plated at a low density at the 4th passage. Bottom:
1286 Quantification of the relative number of AP-positive pluripotent colonies counted per well. Bars
1287 indicate the mean ± SEM of n = 3 independent experiments shown as dots.
1288 **F** Representative gating strategy to evaluate SUSD2 positivity in naive hPSCs by flow cytometry.
1289 Selected sub-populations are shown from left to right. First, the cell population was distinguished from
1290 cell debris (left panel). Singlets were chosen from the cell population and live cells among singlets were
1291 selected, followed by the gating of SUSD2-positive cells using unstained negative control (right panel).
1292 This gating strategy corresponds to Figure 1G and Supplementary Figure 3F.

SUPPLEMENTARY FIGURE 2

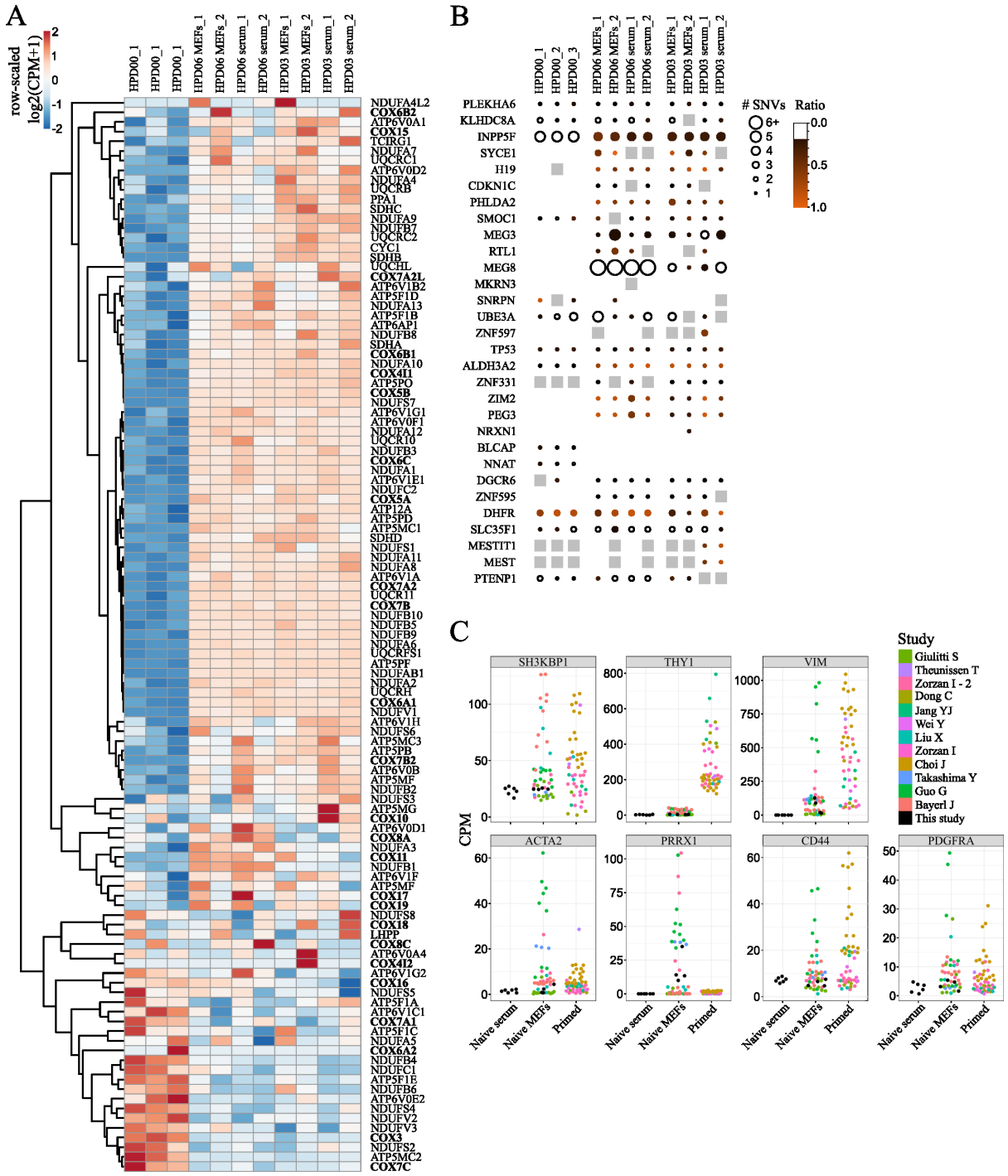

1295 # SUPPLEMENTARY FIGURE 2

1296 **A** Heatmap of oxidative phosphorylation genes from the KEGG PATHWAY Database
1297 (https://www.genome.jp/kegg/pathway.html) and COX genes[24] in HPD00 primed hiPSCs and HPD06
1298 and HPD03 naive hiPSCs stably cultured on MEFs or serum coating.
1299 **B** BrewerIX gene summary panel results on RNA-Seq data from HPD00 primed hiPSCs and HPD06
1300 and HPD03 naive hiPSCs stably cultured on MEFs or serum coating. Empty dots indicate detected
1301 genes with no evidence of biallelic expression, grey squares indicate genes detected but not reaching
1302 the thresholds, and the absence of any symbol indicates that the gene was not detected.
1303 **C** Absolute expression (CPM) of fibroblasts markers from Figure 2D in naive hPSC lines (HPD06 and
1304 HPD03 hiPSCs, and Shef6 hESCs) stably cultured on MEFs or serum coating and in published naive
1305 hPSCs on MEFs and primed hPSCs.

SUPPLEMENTARY FIGURE 3

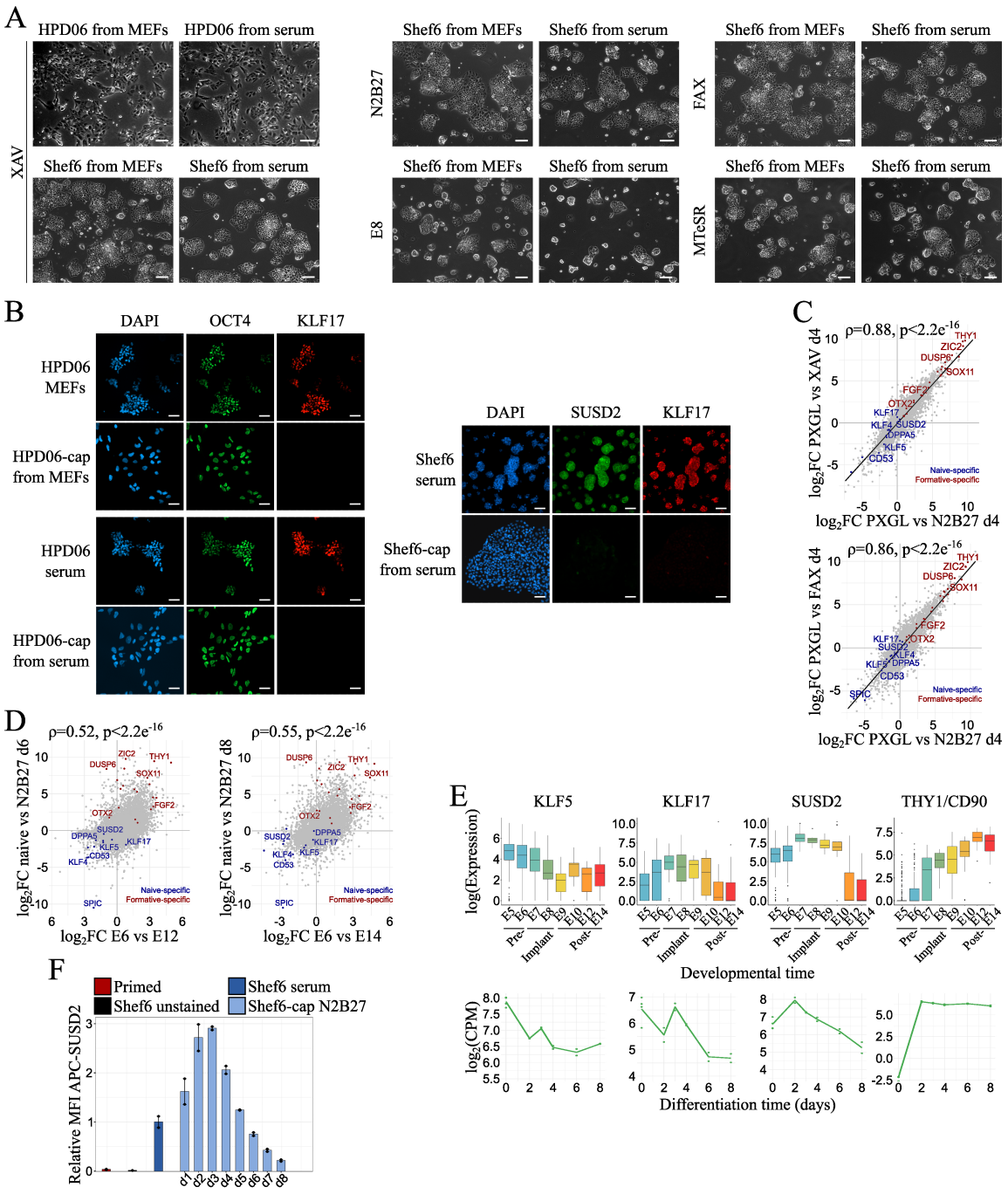

1308 **SUPPLEMENTARY FIGURE 3**

1309 **A** Morphologies of HPD06 hiPSCs and Shef6 hESCs capacitated from naive lines stably cultured on
1310 MEFs or serum coating under different media compositions. Scale bars: 100 µm. Representative images
1311 of two independent experiments are shown.
1312 **B** Immunostaining for general (OCT4) and naive (KLF17 and SUSD2) pluripotency markers of HPD06
1313 hiPSCs and Shef6 hESCs capacitated from naive lines stably cultured on MEFs or serum coating. Scale
1314 bars: 100 µM. Representative images of two independent experiments are shown.
1315 **C** Scatter Plots showing log2 fold changes (log2FC) of Shef6 naive hESCs stably cultured on serum
1316 coating differentiated for 4 days in unsupplemented N2B27 (n = 4 from two independent experiments),
1317 N2B27 supplemented with XAV (n = 2 biological replicates), or N2B27 supplemented with XAV,
1318 FGF2, and Activin A (FAX, n = 2 biological replicates) compared to the naive state (n = 6 from two
1319 independent experiments). Data was filtered for the 9376 DEGs (|log2FC| > 1, padj < 0.05) identified
1320 in any comparison with the naive state. Spearman correlation (ρ, n = 9376) and approximated p-values
1321 are overlaid, with a linear regression line (for visualization) fitted. Selected naive- and primed-specific
1322 markers are labelled.
1323 **D** Scatter Plots showing log2 fold changes (log2FC) of Shef6 naive hESCs stably cultured on serum
1324 coating in the naive state (n = 4 from two independent experiments) versus differentiation for 6 (n = 2
1325 biological replicates) or 8 (n = 2 biological replicates) days in N2B27, compared to corresponding
1326 developmental times (E6 vs. E12 or E14) from the human embryonic reference dataset (subset for
1327 embryonic lineages only)[75]. Data was filtered for the 8508 DEGs (|log2FC| > 1, padj < 0.05) identified
1328 in any comparison between naive hESCs in PXGL and any differentiation timepoint in N2B27, as well
1329 as between E5 or E6 and any later embryonic day until E14. Spearman correlation (ρ, n = 8508) and
1330 approximated p-values are overlaid, with selected naive- and primed-specific genes labelled.
1331 **E** Gene expression of naive (*KLF5*, *KLF17* and *SUSD2*), and primed (*THY1*) pluripotency markers in
1332 the human embryonic reference dataset (subset for embryonic lineages only)[75] and for Shef6 naive
1333 hESCs stably cultured on serum coating differentiated for 6-8 days in N2B27 measured by RNA-seq.
1334 Lines indicate inferred trends based on mean values, with biological replicates (n = 4 from 2
1335 independent experiments for d0, n = 2 biological replicates for any other time point) shown as dots.
1336 **F** Expression of the naive-specific surface marker SUSD2 in Shef6 naive hESCs stably cultured on
1337 serum coating during capacitation for 8 days in N2B27, measured by flow cytometry using an APC-
1338 conjugated anti-SUSD2 antibody. The y-axis represents the relative median fluorescence intensity
1339 (MFI) normalised to the naive state. Bars represent the mean ± SEM of n = 2 biological replicate shown
1340 as dots.

1341 **SUPPLEMENTARY FIGURE 4**

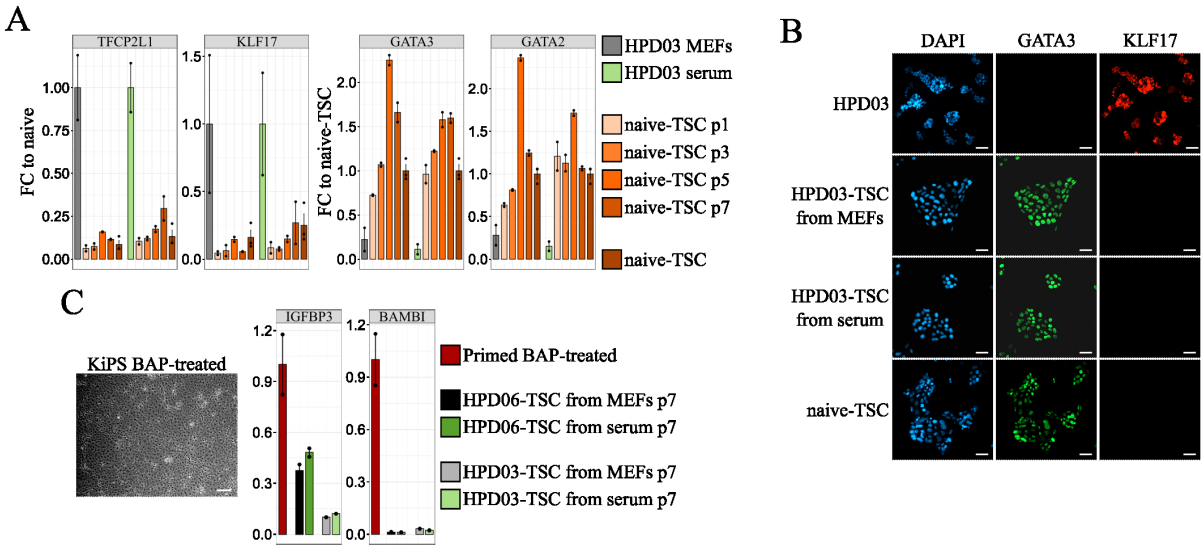

1342

1343 **SUPPLEMENTARY FIGURE 4**

1344 **A** Gene expression analysis by RT-qPCR of naive pluripotency (*TFCP2L1* and *KLF17*) and TSCs
1345 (*GATA3* and *GATA2*) markers in TSCs derived from HPD03 naive hiPSCs stably cultured on MEFs or
1346 serum coating. Bars indicate the mean ± SEM of technical replicates shown as dots. Biological
1347 replicates include n = 3 independent experiments for naive hPSCs and naive-TSCs, and n = 2
1348 independent experiments for the differentiation time points.
1349 **B** Immunostaining for TSCs (GATA3) and naive pluripotency (KLF17) markers in TSCs derived from
1350 HPD03 naive hiPSCs stably cultured on MEFs or serum coating. Scale bars: 100 µM. Representative
1351 images of two independent experiments are shown.
1352 **C** Left: Morphology of KiPS primed hiPSCs treated with BAP medium for 4 days. Scale bar: 100 µm.
1353 Right: Gene expression analysis by RT-qPCR of amnion markers (*IGFBP3* and *BAMBI*) in TSCs
1354 derived from HPD06 and HPD03 naive hiPSCs stably cultured on MEFs or serum coating. Bars indicate
1355 the mean ± SEM of n = 2 biological replicates shown as dots.

SUPPLEMENTARY FIGURE 5

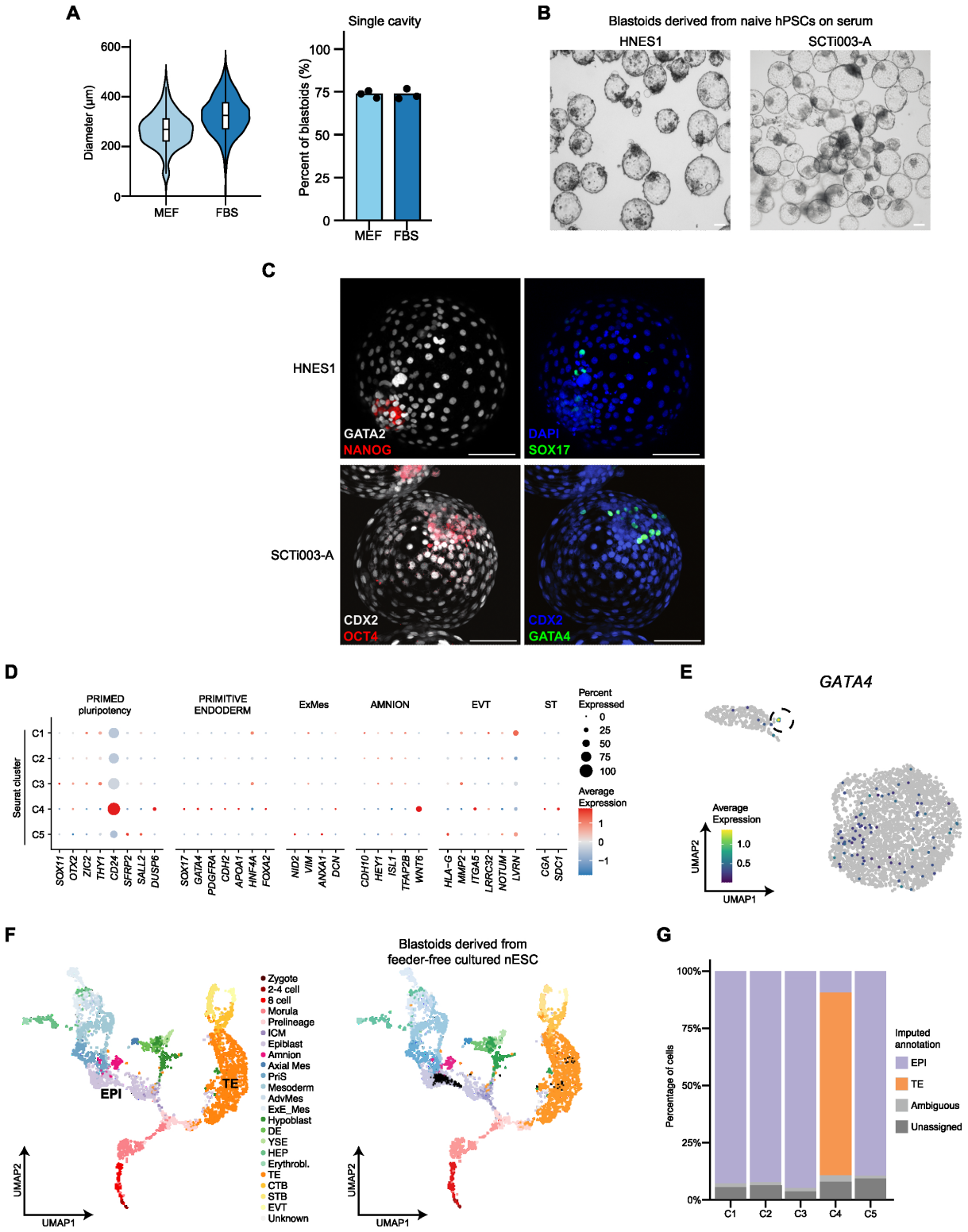

1358 # SUPPLEMENTARY FIGURE 5

1359 **A** Quantification of blastoid diameter (left) and blastoids with a single cavity (right) in structures formed
1360 from naive H9 hESCs cultured on MEFs or serum coating. Left: data is presented as violin plots with
1361 the median, 25, 75 percentiles (± min-max) of n = 407 (MEFs) and n = 806 (serum coating) across 3
1362 biological replicates. Right: Data shows the mean percentages and data points of 3 biological replicates.
1363 **B** Brightfield images of blastoids induced from naive HNES1 hESC and naive SCTi003-A hiPSCs
1364 cultured on serum coating. Scale bar: 100 µm.
1365 **C** Immunostaining of blastoids derived from naive HNES1 hESC and naive SCTi003-A hiPSCs
1366 cultured on serum coating. Blastoids were stained for TE (GATA2 or CDX2), PrE (GATA4 or SOX17)
1367 and EPI (NANOG and OCT4) markers. Shown is the maximum projection. Scale bars: 100 µm.
1368 **D** Expression of selected lineage-specific marker genes across Seurat clusters from Figure 6C. The size
1369 of the dots represents the proportion of cells in the indicated group expressing the given gene and colour
1370 encodes the scaled average expression.
1371 **E** UMAP plot from scRNA-seq analysis as in Figure 6C. Cells are coloured according to *GATA4*
1372 expression (n = 3260).
1373 **F** Left: UMAP of human pre-implantation and post-implantation embryos with annotation for scRNA-
1374 seq data integration from[69] with cells coloured by cell type. Right: Projection of in vivo reference data
1375 with in vitro d5 blastoids from naive H9 hESC cultured on serum coating. Black dots show
1376 neighbourhoods of in vitro generated cells projected onto a reference UMAP.
1377 **G** Imputed cell annotation across different Seurat clusters as in Figure 6F. Unassigned and ambiguous
1378 labels refer to cells with either none or with more than two imputed stages respectively.